CHAPTER 5

CASE STUDY OF THE FORT ST. JOHN GRABEN AREA

The deltaic sandstones of the basal Kiskatinaw Formation (Stoddart Group, upper Mississippian) were preferentially deposited within structural lows in a regime characterized by faulting and structural subsidence. In the case study of the Fort St. John Graben area, northwest Alberta, Canada, these sandstone facies can form reservoirs where they are laterally sealed against the flanks of upthrown fault blocks. Exploration for basal Kiskatinaw reservoirs generally is accompanied by the acquisition and interpretation of surface seismic data prior to drilling. These data are used to map the grabens in which these sandstones were deposited, and the location of horst blocks which act as lateral seals. Subsequent to drilling, three vertical seismic profile (VSP) surveys were conducted at the 9-24-82-11 W6M exploratory well site. These data supplemented the surface seismic and well log control such that (Hinds et al., 1991a; Hinds et al., 1993a; Hinds et al., 1994c):

1) direct correlation is made with the surface seismic data. As a result, the surface seismic control was accurately tied to the subsurface geology and geological seismic markers;

2) multiples were positively identified on the VSP data and the effect of these events on the surface seismic interpretation was determined; and

3) the subsurface geology, in the vicinity of the borehole, is more clearly resolved on the

VSP data than on the surface seismic control and an investigation of the basal Kiskatinaw revealed amplitude anomalies and local faulting which was not evident on the surface seismic data (Hinds et al., 1994b).

This chapter is a case history of the Fort St. John Graben 9-24 well (as reported in Hinds et al., 1991a; Hinds et al., 1993a and 1994b). An overview of the stratigraphy (Fig. 5.1) and the geologic history of the Lower Carboniferous in the study area is included. The acquisition and interpretive processing of the VSP data is described, and an integrated interpretation of the well log, surface seismic and seismic profile data is presented.

On the Fort St. John Graben dataset described in this chapter, faults which are not well resolved on the surface seismic data are better delineated on the VSP data. The interpretive processing of these data illustrate the utility of the seismic profiling technique to the search for hydrocarbons in structurally complex areas.

5.1 Introduction

On the basis of conventional surface seismic data, an exploratory well (9-24-82-11 W6M) was drilled into the basal Kiskatinaw Formation (Stoddart Group, upper Mississippian; Fig. 5.1) on the downthrown side of a fault block in the Fort St. John Graben area, Peace River Embayment (Fig. 5.2 and 5.3). It was expected that gas-prone sandstones of the basal Kiskatinaw would be laterally truncated and sealed against shales of the Golata Formation. Contrary to expectations, the well encountered unproductive, shaly sandstone tidal-flat facies

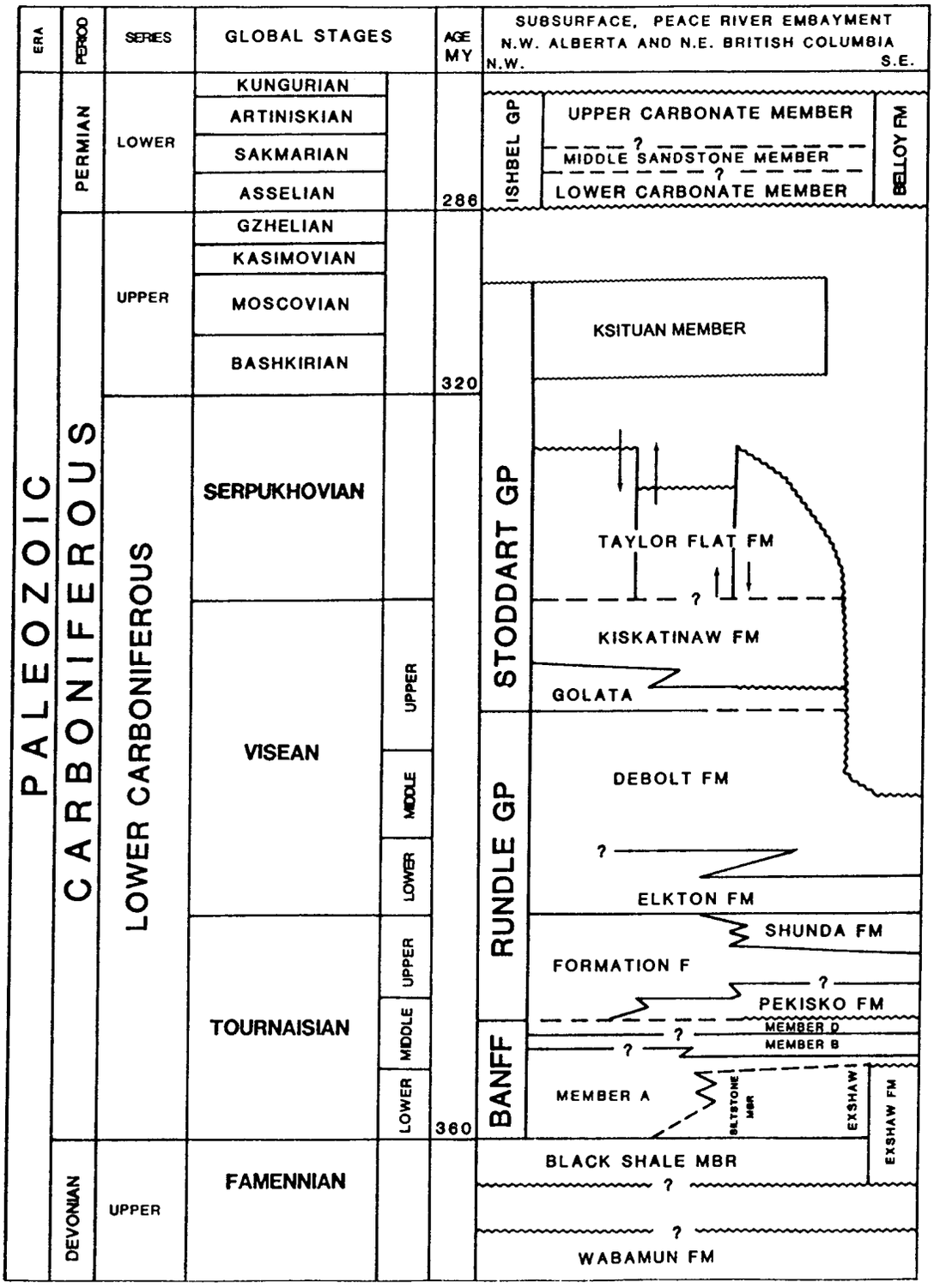

Figure 5.1 Stratigraphy of the Fort St. John Graben study area (modified from Richards, 1989).

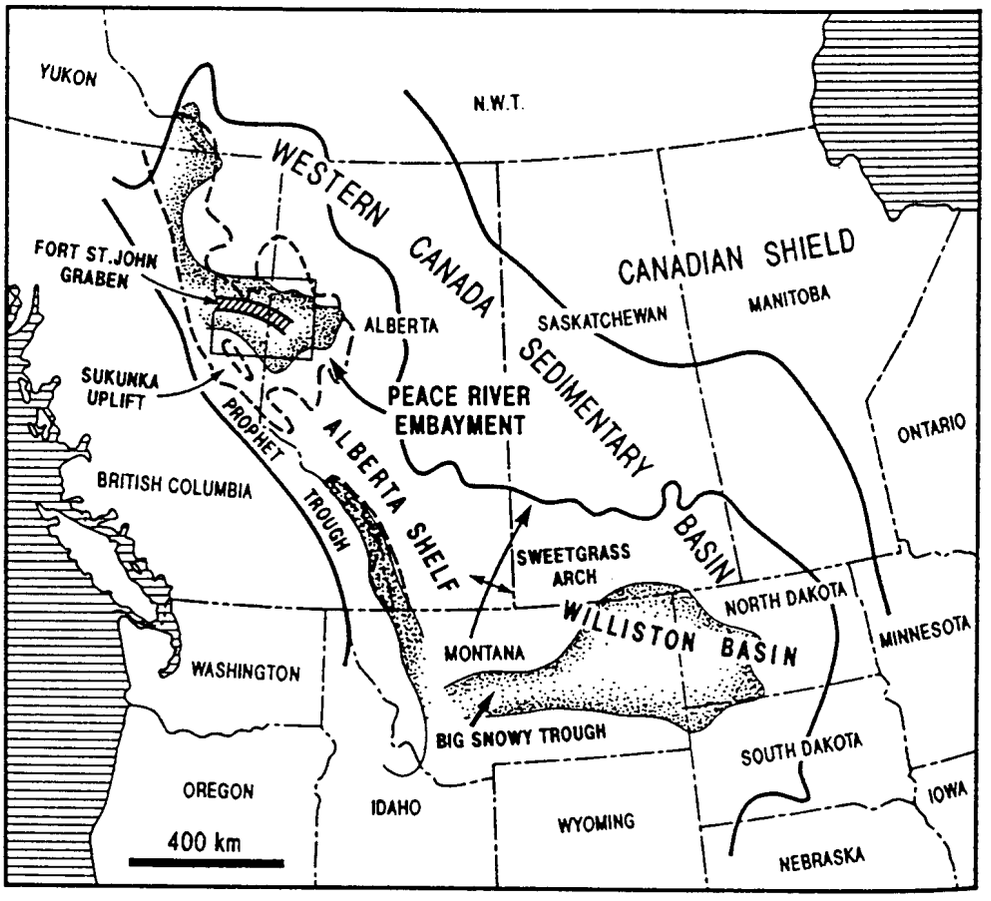

Figure 5.2 Map of Western Canadian Sedimentary Basin tectonic elements showing the Peace River Embayment, Prophet Trough, Sukunka Uplift, cratonic platform and Fort St. John Graben. (Barclay et al., 1990)

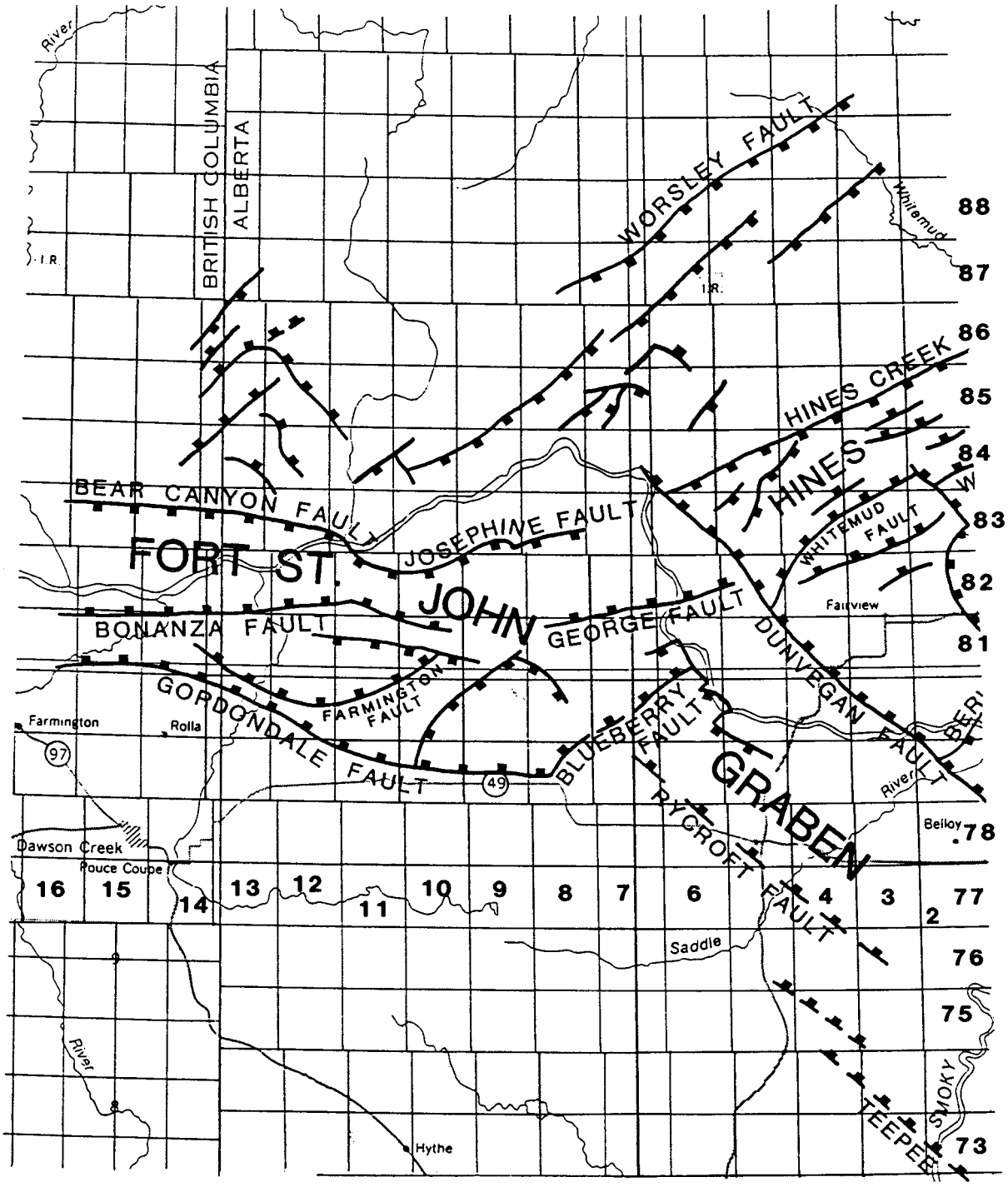

Figure 5.3 Detailed area map of the Fort St. John Graben showing the Bear Canyon, Josephine, Bonanza and George faults (from Richards et al., 1994). The study area is centred in Township 82 and Range 11 west of the 6th Meridian in Alberta, Canada near the Alberta and British Columbia provincial border.

in the basal Kiskatinaw and a commercial gas-bearing zone in the upper Kiskatinaw, and is now shut-in (Hinds et al., 1991a; Hinds et al., 1993a and 1994b).

To obtain a higher resolution image of the subsurface in the vicinity of well 9-24, and to evaluate the presence and proximity of any fault features which might not have been resolved on the surface seismic data, three VSP (vertical seismic profile) surveys were designed and performed at the 9-24 well site. These profiles were used in conjunction with surface seismic coverage to cooperatively image the fault systems in the area and to elucidate the seismic signature of the upper Kiskatinaw reservoir which had not been prognosed.

5.2 Geological overview

5.2.1 Tectonic and depositional history of the Peace River Embayment

This section will review the tectonic and depositional history for the study area. Unlike the case studies of chapters 3, 4, and 6 which pertain to carbonate reef exploration in the WCSB; this case study pertains to channel sand deposition and hydrocarbon entrapment within. The following section will review the stratigraphy of the study area.

Investigation of the Peace River Arch and Peace River Embayment revealed a depositional regime characterized by faulting (O'Connell, 1990) and structural subsidence. The Peace River Arch can be traced to a crustal structure consisting of uplifted granitic basement (Fig. 5.4a; Cant , 1988) and subsequently was deformed in three main phases:

1) the formation of a structural high in the latest Late Proterozoic which was onlapped by siliciclastic, evaporite and carbonate deposition until the Middle to Late Devonian;

The basement was uplifted 800 to 1000 m above the regional elevation (Cant, 1988) during the early Paleozoic (mid-Cambrian) as an asymmetrical feature with the northern flank dipping steeply and the southern flank dipping more gently (O'Connell et al., 1990). During the Middle to Upper Devonian, a diachronous siliciclastic unit (lithozone as defined in Trotter, 1989) called the Granite Wash (sediments derived from plutonic and metamorphic basement relics) and carbonate and shale deposits of the Elk Point (along with Gilwood sandstone), Beaverhill Lake (Slave Point, carbonate reefs and Waterways Fm) , Woodbend (fringing reefs, basal ramp to stacks of carbonate shelves and overlying carbonate ramp) and Winterburn (Nisku and Blueridge Fm; Moore, 1988) Groups onlapped onto the emergent arch. The Wabamun Fm carbonates eventually buried most of the Arch. Another feature existing during the deposition of the Wabamun Fm was localized islands of subaerially exposed Granite Wash Fm that were present during the deposition of the lower Banff Fm (Richards, 1991, pers. comm.).

2) the formation of a series of embayments resulting in anomalously thick Carboniferous, Permian and Triassic deposits;

During the deposition of the Middle Devonian Elk Point Group, normal faulting began. These normal faults were rejuvenated in the late Famennian during the deposition of the upper Wabamun Fm and the overlying Exshaw Fm (Fig. 5.4b).

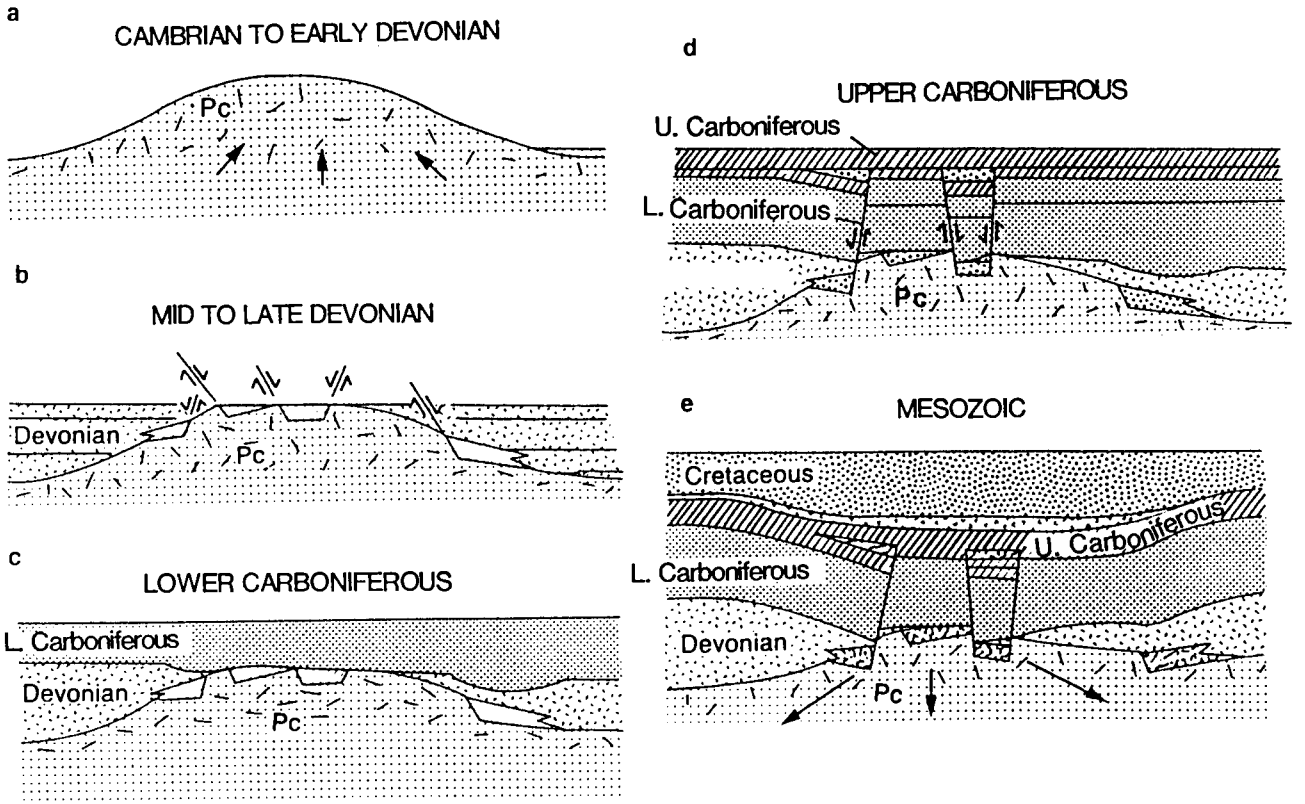

Figure 5.4 Diagrammatic summary of the depositional and tectonic history of the Peace River Embayment area (from Cant, 1988) from the Cambrian to the Cretaceous periods.

3) the development of a deep basin component of the foreland basin during the Jurassic and Cretaceous.

The arch ceased to be emergent by the beginning of the Carboniferous.

The Peace River Embayment, a structural inversion consisting of northeast to southwest trending interlinked graben and half-grabens (Barclay et al., 1990), started to develop during the latest Devonian (late Famennian) and earliest Carboniferous when the Exshaw and overlying lower Banff Fm were deposited (Richards, 1989; Richards et al., 1994). The major tectonic features surrounding the Embayment were the Prophet Trough (Richards, 1989; Richards et al., 1994), Sukunka Uplift (Richards, 1989) and cratonic platform (Fig. 5.2). The northwest-trending narrow pericratonic Prophet Trough (O'Connell et al., 1990) resulted from the downwarping and downfaulting of the western margin of the North American plate during the latest Devonian (late Famennian) and Carboniferous and is interpreted as a back-arc basin (Richards, 1989). In the detailed stratigraphic correlation chart (Fig. 5.1), the Famennian to Tournaisian boundary coincides with the Devonian to Carboniferous boundary. The Carboniferous Peace River Embayment opened northwestward into the Prophet Trough. During the middle to late Tournaisian, the Embayment became better defined as a separate entity. The northern Sukunka uplift on the southwestern side of the Embayment formed a low rim that restricted the access of the Embayment sediments into the southeastern part of the Prophet Trough.

Regional subsidence continued associated with extensive block faulting (Fig. 5.4d) along normal faults (Cant, 1988). During the period of block faulting, anomalously thick Lower

Carboniferous successions of siliciclastics and ramp-to-platform carbonates were deposited along the axis of the embayment (Richards, 1989, 1990).

The Devonian and Carboniferous tectonic history of the Peace River Embayment has been summarized by Richards (1989, 1990) and Richards et al. (1994). The onset of its development is postulated to be the late Famennian to early middle Tournaisian. During that initial time, the deposition of the Exshaw Fm and the overlying lower Banff Fm occurred (Richards, 1990).

5.2.2 Lower Carboniferous: Fort St. John Graben Area

Within the Carboniferous succession in the Fort St. John Graben study area (Fig. 5.3), four principal episodes of blockfaulting have been recognized (Richards 1989, 1990):

1) after deposition of the latest Devonian to earliest Carboniferous deposits of the Exshaw Fm but prior to the deposition of the overlying Banff Fm;

2) during deposition of the lower Banff Fm (early middle Tournaisian);

3) during the deposition of the Golata and Kiskatinaw Formations (late Visean); and

4) after deposition of the upper Visean to Serpukhovian (?) Taylor Flat Fm but prior to that of the Permian Ishbel Group.

Marked regional subsidence accompanied the second and third phases of blockfaulting, whereas subaerial erosion and local uplift accompanied the first and last phases. Pronounced regional subsidence, at least locally, accompanied by blockfaulting also took place during deposition of the middle and upper Tournaisian Pekisko and Shunda Formations. In the middle Tournaisian, the developed embayment can best be termed a deep re-entrant into the western cratonic platform and the Prophet Trough is interpreted as a back arc basin (Richards, 1989). Deep-water environments existed in the embayment area during periods of pronounced subsidence. In the general study area, the Fort St. John and Hines Creek Grabens (Barclay et al., 1990) were already developing before the deposition of the Stoddart Group.

The Lower Carboniferous deposition spans from the upper part of the Exshaw Fm to the top of the Taylor Flat Fm. Carbonate and fine-grained terrigenous clastics were deposited during the Exshaw-Debolt interval. Basal shale, carbonate ramp deposits, shallow water shelf carbonates, inter- to supratidal carbonate, clastics and evaporites were deposited in the Banff Fm. Shales are also found in the Pekisko Fm, a coeval correlative for the Pekisko and Shunda defined in Richards (1989) called Formation F and Shunda Fm which overlie the Banff Fm. A well developed basin, slope and shelf environment in the Peace River Embayment was developed during the deposition of the lower and middle Banff Fm and during the Pekisko/Shunda succession. Apart from these times, sedimentation in the area kept pace with the subsidence which resulted in normal topographic relief.

The Golata, Kiskatinaw and Taylor Flat Formations were deposited in the late Visean and Serpukhovian subsequent to the deposition of the Debolt Fm with the Golata overlying the

Debolt Fm conformably in the central part of the embayment. The Golata consists of fissile grey mudstone, siltstone and shale (Barclay, 1988). Towards the basin margins, the Golata and Debolt contact becomes disconformable (O'Connell et al., 1990).

The Kiskatinaw consists predominately of sandstone with minor quantities of fine grained siliciclastics, limestones, dolostones and coals. At least eight depositional cycles make up the formation, but three main depositional cycles are referred to informally as the lower, middle and upper Kiskatinaw. The Kiskatinaw Fm represents a marine-dominated deltaic system which may have resembled an estuary in the study area during deposition (Richards, 1989; Richards et al., 1994). The study area was a semi-enclosed body of coastal water. Blockfaulting occurred accompanied by deep subaerial erosion which resulted in substantial thickness changes in the Kiskatinaw and Taylor Flat Fm deposits.

The Kiskatinaw and Golata Fm contact is unconformable. This prodelta sequence (Golata Fm) can serve as a reservoir seal in those places where, as a result of faulting, it is juxtaposed against the sandstones of the basal Kiskatinaw. The uppermost and basal Kiskatinaw Fm sandstones deposits are exploration targets.

The deposition in the study area is shown in the models for the Stoddart Group deposition in figure 5.5a-d (from Barclay et al., 1990; Fig. 17a-d). The creation of the hydrocarbon trapping structures occurred prior to the deposition of the Permian Belcourt and Belloy Fm.

The study area is in the Fort St. John Graben area defined by East-West faulting to the North

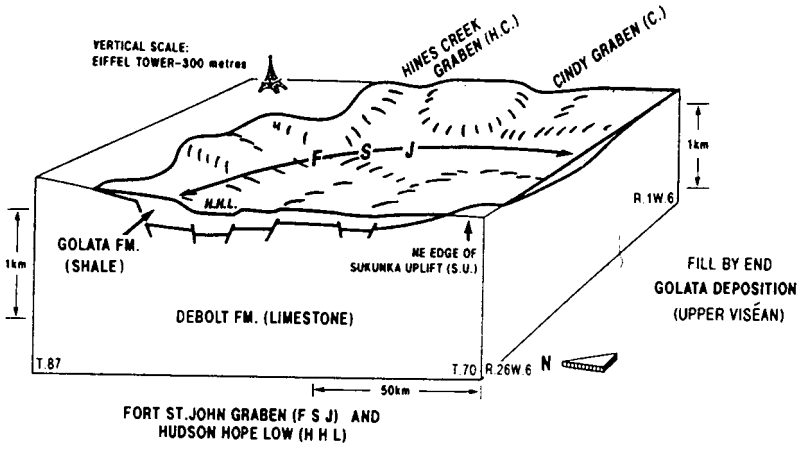

Figure 5.5A Block diagram showing the Fort St. John Graben deposition by the end of the Golata Formation time (from Barclay et al., 1990).

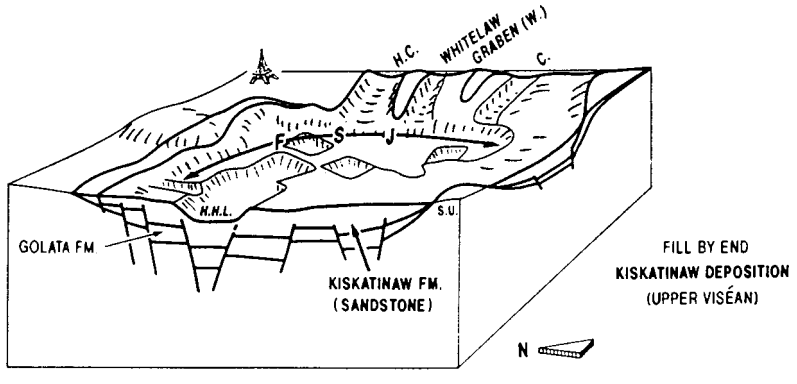

Figure 5.5B Block diagram showing the Fort St. John Graben deposition by the end of the Kiskatinaw Formation time (from Barclay et al., 1990).

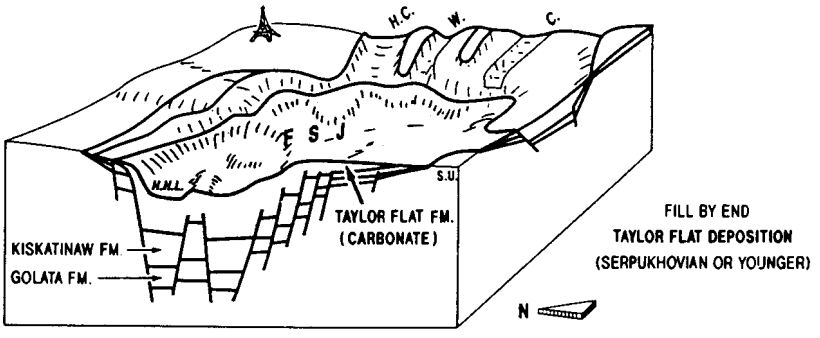

Figure 5.5C Block diagram showing the Fort St. John Graben deposition by the end of the Taylor Flat Formation time (from Barclay et al., 1990).

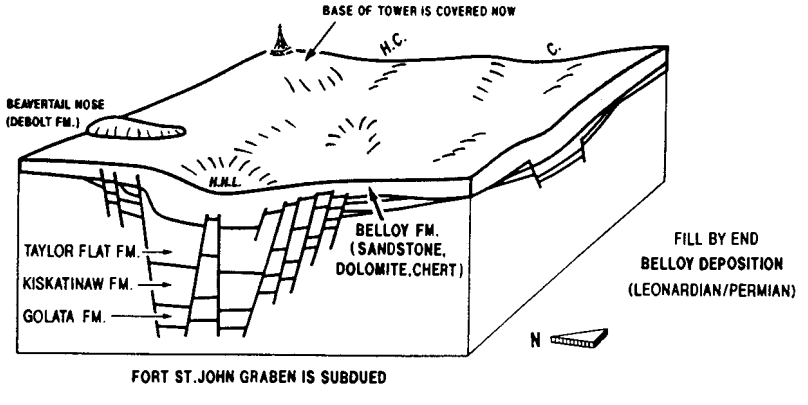

Figure 5.5D Block diagram showing the Fort St. John Graben deposition by the end of the Belloy Formation time (from Barclay et al., 1990).

(Bear Canyon and Josephine faults) and to the South (Bonanza fault) as shown in Figure 5.3. The Fort St. John Graben is part of the Dawson Creek Graben Complex (Barclay et al., 1990) as is shown in figure 5.6 and 5.7.

The channel fill making up the basal Kiskatinaw (Barclay, 1988) were the target of the 9-24 well. The hypothesis was that thick sections of basal Kiskatinaw would be preferentially deposited in the structural lows on the downthrown side of early Kiskatinaw faults. The basal Kiskatinaw encountered by the 9-24 well was not of reservoir quality; however, the sandstones of the upper Kiskatinaw contain commercial gas.

5.3 Original interpretation and well results

Seismic data interpreted by the owners of the well prior to the drilling of well 9-24 and the running of the VSP surveys are shown in Figure 5.8. All subsequent interpretation on data presented within this chapter are presented as part of the thesis research.

The split-spread, 96 pre-stack trace data used to create the stacked section (Fig. 5.8) were acquired using a patterned dynamite source (3 X 3 kg at 15 m) and DFS4 recording equipment (12/18-124 Hz filter; notch (60 Hz) filter out). The groups consisted of nine inline 14-Hz L25D geophones spaced at 6.1 m. The geophone group, shot, common mid-point (CMP), and near offset intervals were 67.1, 134.1, 33.5, and 201.2 m respectively.

The seismic section (normal polarity display; Fig. 5.8) was migrated using a prestack partial

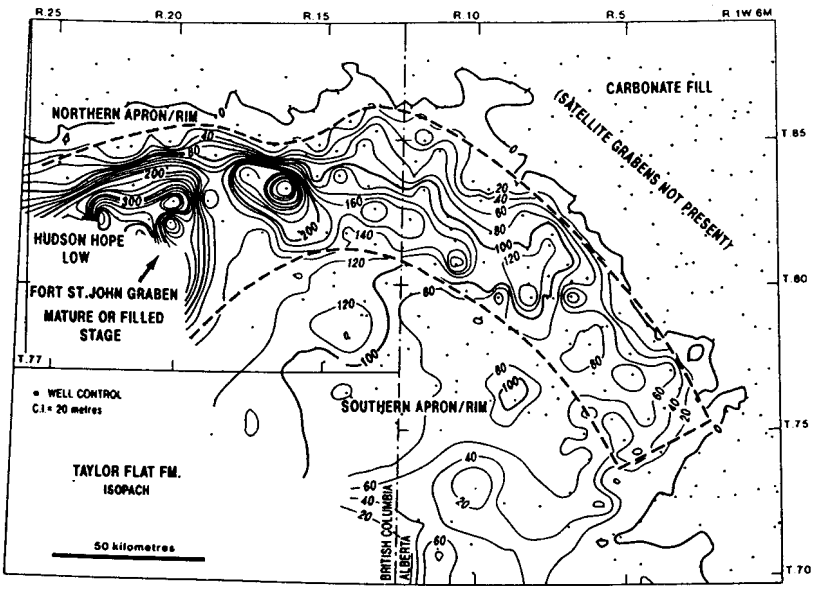

Figure 5.6 Location of the Fort St. John Graben as outlined by the Belloy Formation isopach map (from Barclay et al., 1990). The Belloy deposition marked the end of the subsidence in the graben.

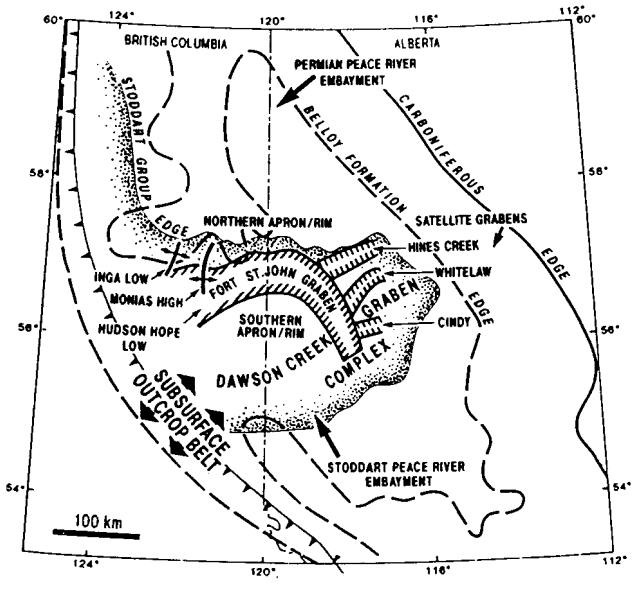

Figure 5.7 Peace River Embayment stratotectonic elements including the Fort St. John Graben (from Barclay et al., 1990).

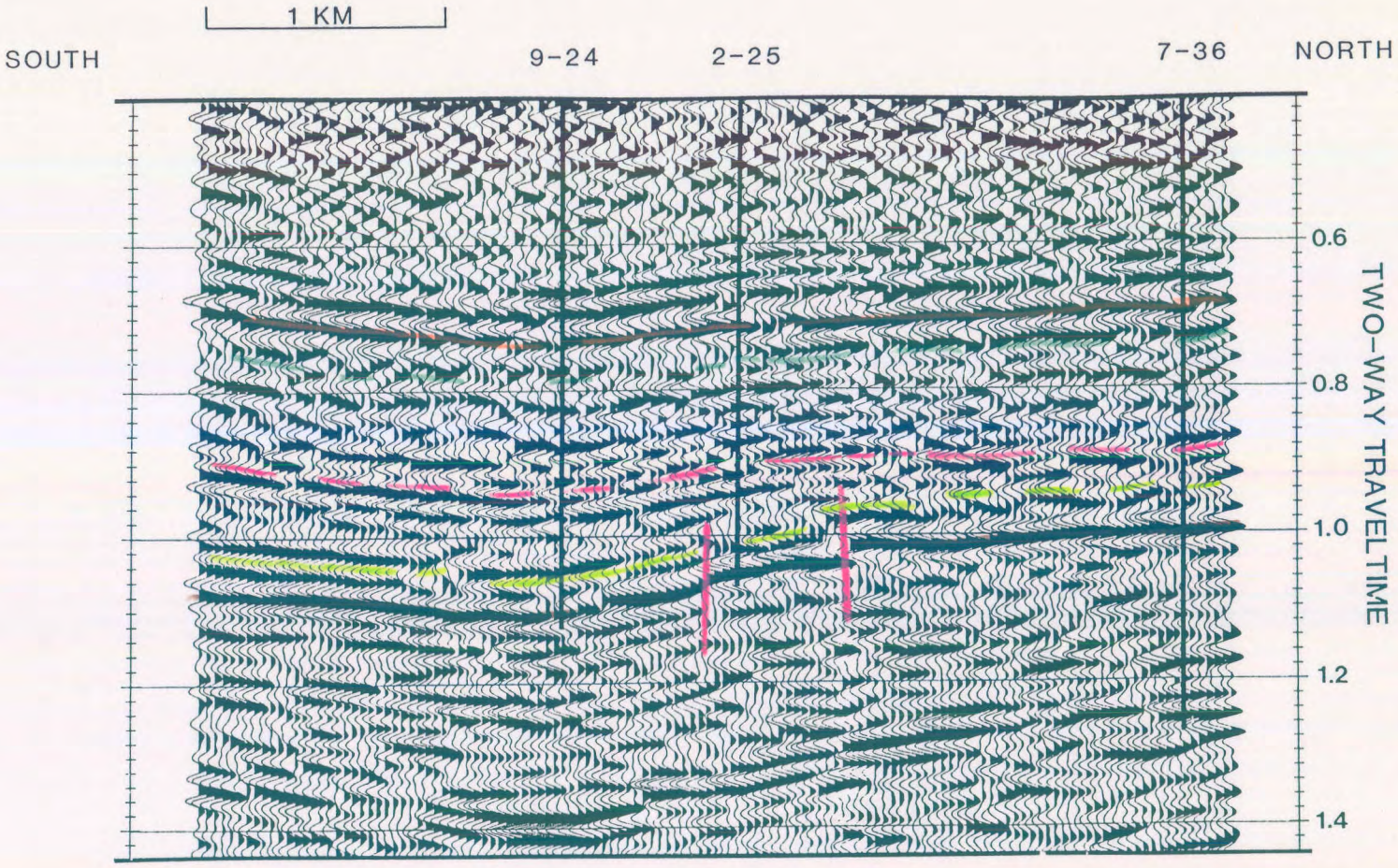

Figure 5.8 Example surface seismic data displaying the original interpretation of the owners of the 9-24 well (preceding the drilling of the well). The data suggested one major fault between the intended well 9-24 and the existing well 2-25.

migration scheme which consisted of applying a common-offset domain, dip-moveout (DMO) correction (Hale, 1984) to the prestack data. Updated velocities were then determined using the DMO-corrected CMP gathers. Closely spaced velocity analyses were performed since the stacking velocities changed rapidly along the line. This prestack processing was followed by poststack phase-shift migration. The poststack migration method is reviewed in Gazdag (1978) and Gazdag and Squazzero (1984).

The surface seismic data were used to elucidate the structural setting at the Kiskatinaw level. The interpreted events on the seismic line are the Nordegg, Halfway/Doig, Belloy, basal Kiskatinaw, and Debolt (stratigraphically listed in Fig. 5.1). The 9-24-82-11 W6M well was located approximately 200 m east of the seismic line and has been projected onto the seismic line as shown in Figure 5.8. Note that 9-24, as projected, is on a downthrown fault block relative to 2-25-82-11 W6M and 7-36-82-11 W6M (Fig. 5.8).

Well 2-25 encountered approximately 25 m of relatively clean, wet basal Kiskatinaw sandstone and was abandoned. Well 7-36 penetrated 35 m of basal Kiskatinaw sandstone which tested gas plus salt water and is currently classified as a shut-in gas well. Well 9-24 was drilled in the expectation that basal Kiskatinaw gas would be stratigraphically entrapped against the flank of the upthrown flank block; however the basal Kiskatinaw proved to be shaly-sandstone and not of reservoir quality. 9-24 was shut-in as an upper Kiskatinaw gas well.

5.4 VSP acquisition

Three VSP surveys were run at the 9-24 well site (one near offset and two far offset sources). The VSP were planned with the following objectives in mind:

1) to provide a confident surface seismic tie to:
   a) the upper Kiskatinaw Fm reservoir;
   b) the lower Kiskatinaw Fm; and
   c) the Debolt Fm;

2) to determine if multiple reflections were a significant problem at the Kiskatinaw level, and to design an effective deconvolution filter;

3) to map the lateral extent of the shaly sandstone of the basal Kiskatinaw and upper Kiskatinaw reservoir in the direction of the far offset VSPs; and

4) to provide a higher resolution seismic image of the Debolt fault in the vicinity of the 9-24 well.

The near offset VSP source was located 149 m from well 9-24 and in the direction of well 2-25. One of the far offset source locations (referred to as FSJG1 in chapter 2) was in the direction of 2-25 and 700 m from the 9-24 well site. The other far offset source location (referred to as FSJG2) was situated 741 m east of well 9-24. Two Vibroseis units operated

in series at each offset using a 12 second sweep of 10-90 Hz. The recording length was 15 seconds resulting in a 3 s cross-correlated output. On average, six sweeps were summed at each geophone sonde location. The total depth of well 9-24 was 2126 m below Kelly Bushing of the drilling rig (KB at 644 m asl). All three offset sources were at 639 m asl. Data were recorded at a sampling rate of 1 ms using an MDS-10 unit. The recording filter, OUT/250, was designed to prevent aliasing.

The triaxial sonde vertical spacing was 20 m (from a depth of 2030 m up to 350 m). As a precautionary measure, calibration records were acquired at several depths as the sonde was lowered down the borehole and repeated again during the production runs to detect possible depth errors or cable stretch.

5.5 Near offset (149 m) VSP interpretive processing

During the processing of the near offset VSP data, a series of interpretive processing panels (IPPs) were designed. These panels were designed to display the following interpretive processing steps (Hinds et al. 1991a; Hinds et al., 1993a and 1994b; and Hinds et al., 1994c):

1) upgoing and downgoing P-wave separation;

2) deconvolution of the separated upgoing P-waves; and

3) inside and outside corridor stacks of both the nondeconvolved and deconvolved upgoing waves.

5.5.1 P-wave event separation

The separation of the upgoing and downgoing P-waves from the Z(FRT) data is displayed in the wavefield separation interpretive processing panel (Hinds et al., 1989a; Hinds et al., 1993a; Hinds et al., 1994c) of Figure 5.9.

Panel 1 displays the Z(FRT) data after trace normalization. The upgoing P-wave events are difficult to discern until the Z(FRT) data are gained (panel 2). On these panels, the tube wave is visible below 0.9 s as a high-frequency, downgoing wavetrain with a velocity of propagation of about 1435 m/s. The tube wave reflects from the bottom of the well borehole and travels back up. This accounts for the upgoing tubewave F-K events discussed in chapter 2.

Several upgoing primary events and multiple reflections can be identified on panel 2. Consider for examples, the Spirit River and Nordegg events which are highlighted in blue and orange, respectively. Each of these events is followed by a trailing surface-generated multiple with a lag time of about 110 ms. This multiple pattern (both upgoing and downgoing waves) is highlighted in panel 2 of Figure 5.9.

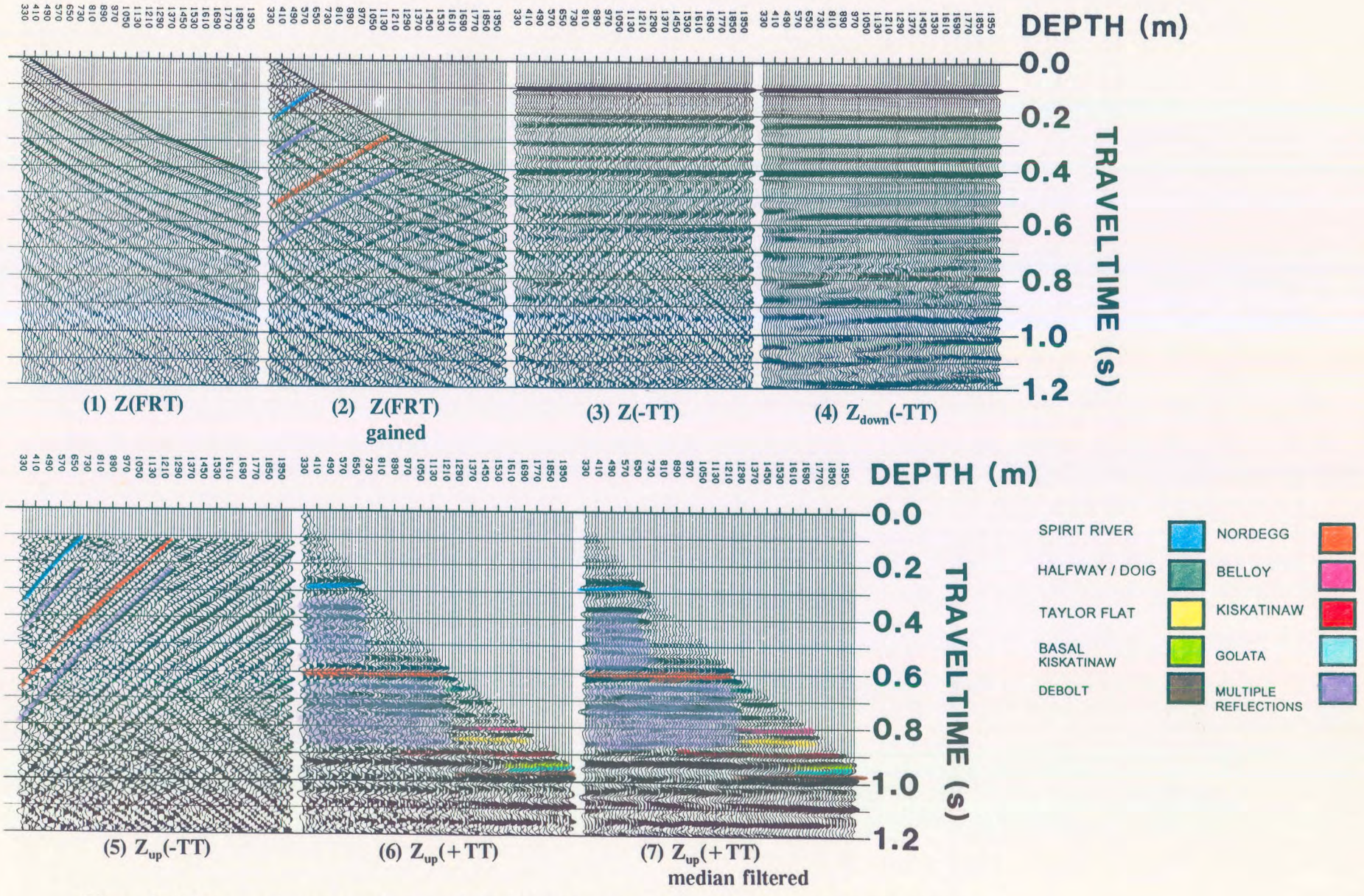

Figure 5.9 Interpretive processing panel depicting the wavefield separation of the near offset Fort St. John Graben VSP data (from Hinds et al., 1993a).

In panel 3 (Fig. 5.9), the **Z(-TT)** data are displayed. An 11-point median filter was used to remove the upgoing P-waves; the $\mathbf{Z_{down}(-TT)}$ data are displayed in panel 4. In the next step, the $\mathbf{Z_{down}(-TT)}$ data of panel 4 were subtracted from the **Z(-TT)** data to yield the $\mathbf{Z_{up}(-TT)}$ data (panel 5). Note that a residual tube wave is visible within the $\mathbf{Z_{up}(-TT)}$ data panel.

The $\mathbf{Z_{up}(+TT)}$ data before and after the application of a 3 point median filter are shown in panels 6 and 7, respectively. The two panels have been time shifted to facilitate plotting. In panel 7, the Spirit River multiple (highlighted in panel 2) is observed as high amplitude events which lie directly below the Spirit River primary and can be interpreted for several cycles (from 0.3 to 0.7 s). This multiple is not observed at sonde depths deeper than the top of the Spirit River (at 730 m).

5.5.2 Near offset VSP deconvolution

Deconvolution IPP (Hinds et al., 1989a) were designed for the $\mathbf{Z_{up}(+TT)}$ data (Fig. 5.10) to enable the monitoring of the deconvolution process for the near offset data (Hinds et al., 1993a; Hinds et al., 1994c). The incorporated panels reveal information (about multiples) that was difficult to determine from the wavefield separation IPP (Fig. 5.9) alone. The first two panels (Fig. 5.10) are the nonfiltered and median-filtered $\mathbf{Z_{up}(+TT)}$ data, respectively. The interpreted multiple events have been highlighted in purple on panels 1 and 2.

Panel 3 is the gained $\mathbf{Z_{down}(-TT)}$ data. Panels 4 and 5 are the nondeconvolved and deconvolved $\mathbf{Z_{up}(-TT)}$ data, respectively, which enable an evaluation of the effect that the deconvolution process has on the $\mathbf{Z_{up}(-TT)}$ data.

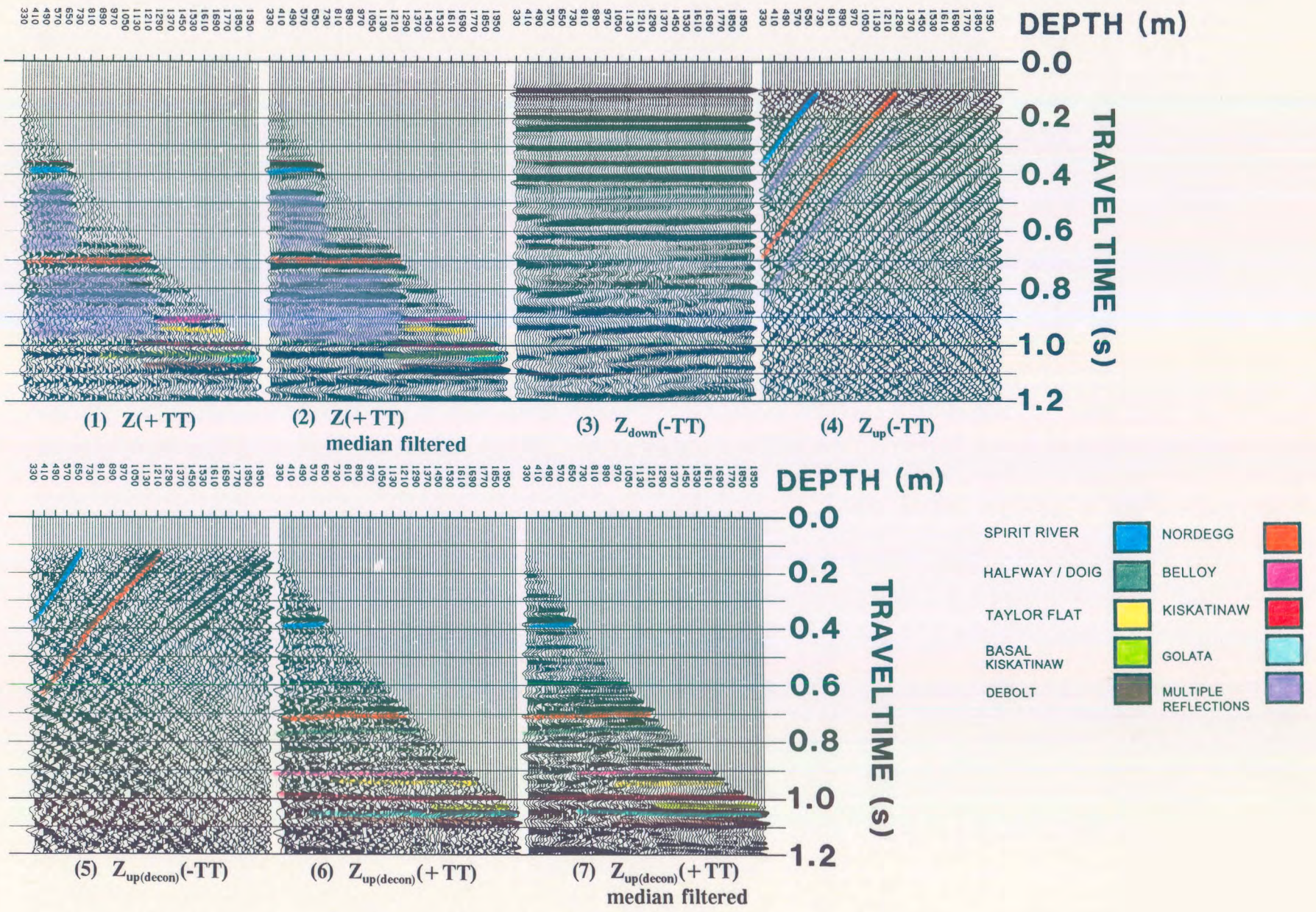

Figure 5.10 Interpretive processing panel depicting the deconvolution of the near offset Fort St. John Graben VSP data (from Hinds et al., 1993a).

The last two panels (6 and 7) are the nonmedian and median-filtered $\mathbf{Z_{up(decon)}(+TT)}$ data, respectively. By inspection of panels 2 and 7 (Fig. 5.10), it is interpreted that the deconvolution processing has effectively attenuated multiple reflections. The Spirit River multiple wavetrain from 0.5 to 0.9 s on panel 2, for example (coloured in purple), has negligible amplitude on panel 7. Note also that deconvolution has increased the frequency content of the data, allowing for better resolution at the Kiskatinaw level.

5.5.3 Inside and outside corridor stacks

Nondeconvolved, inside and outside corridor stacks and associated displays (Hinds et al., 1989a) were designed for the near offset data as presented in Figure 5.11 (Hinds et al., 1993a; Hinds et al. 1994c). A comparison of the inside and outside corridor stacks (panels 3 and 4, respectively) illustrates the utility of these displays. For example, the Spirit River multiple (between 0.65 and 1.0 s) is present on the inside corridor stack and absent on the outside corridor stack. Note also, that basal Kiskatinaw and Golata events can be resolved on the outside corridor stack; on the inside corridor stack these reflections are masked by a high-amplitude multiple.

If deconvolution is successful, the deconvolved inside and outside corridor stacks (panels 3 and 4; Fig. 5.12) should be similar . At the zone of interest just above 1.35 s, the Debolt and the Golata are similar (panels 3 and 4), however the basal Kiskatinaw is not adequately represented on the inside corridor stack of the deconvolved data. An examination of the input data to the inside corridor stack (panel 2 of Fig. 5.12) reveals that the multiple

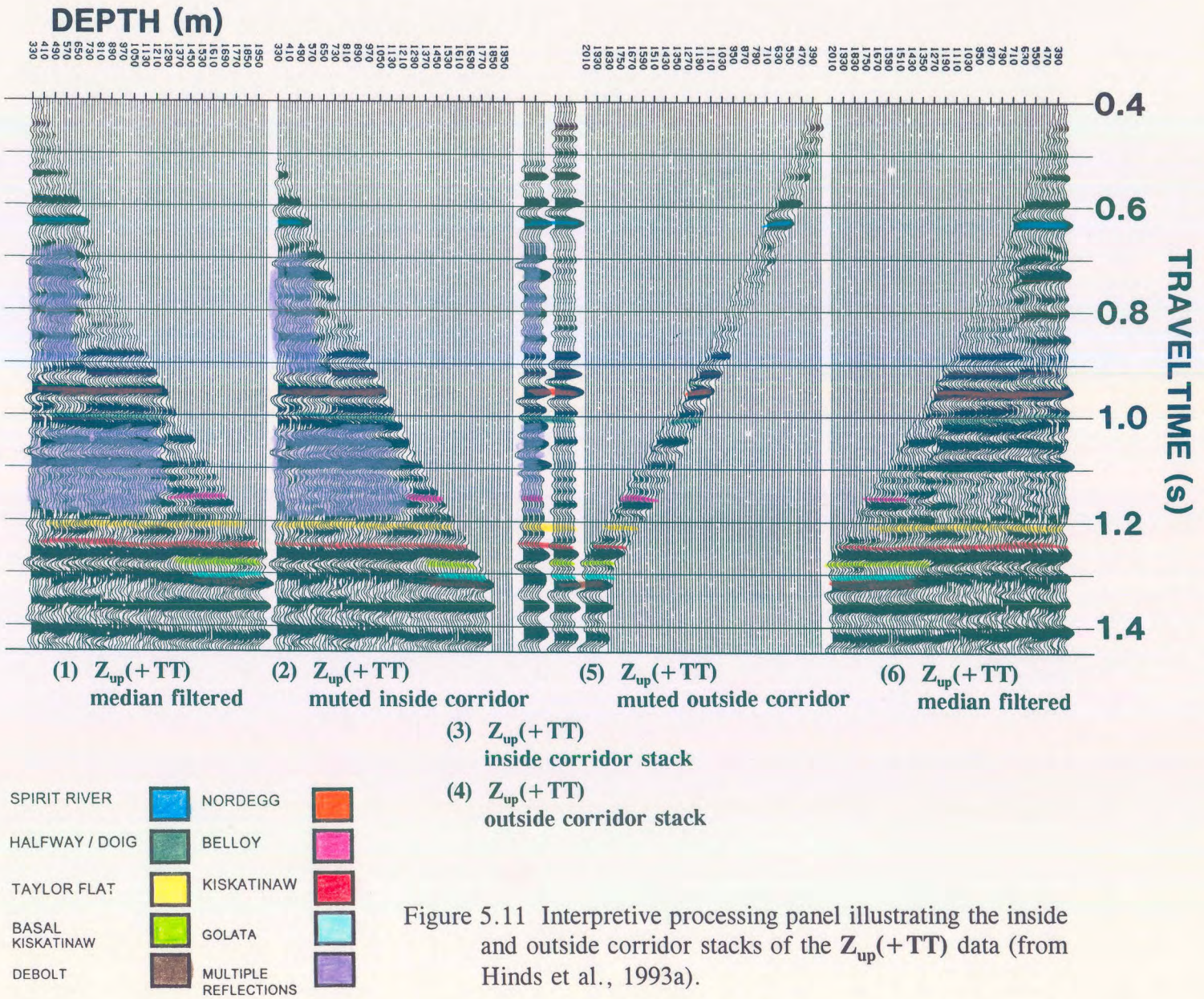

Figure 5.11 Interpretive processing panel illustrating the inside and outside corridor stacks of the $Z_{up}(+TT)$ data (from Hinds et al., 1993a).

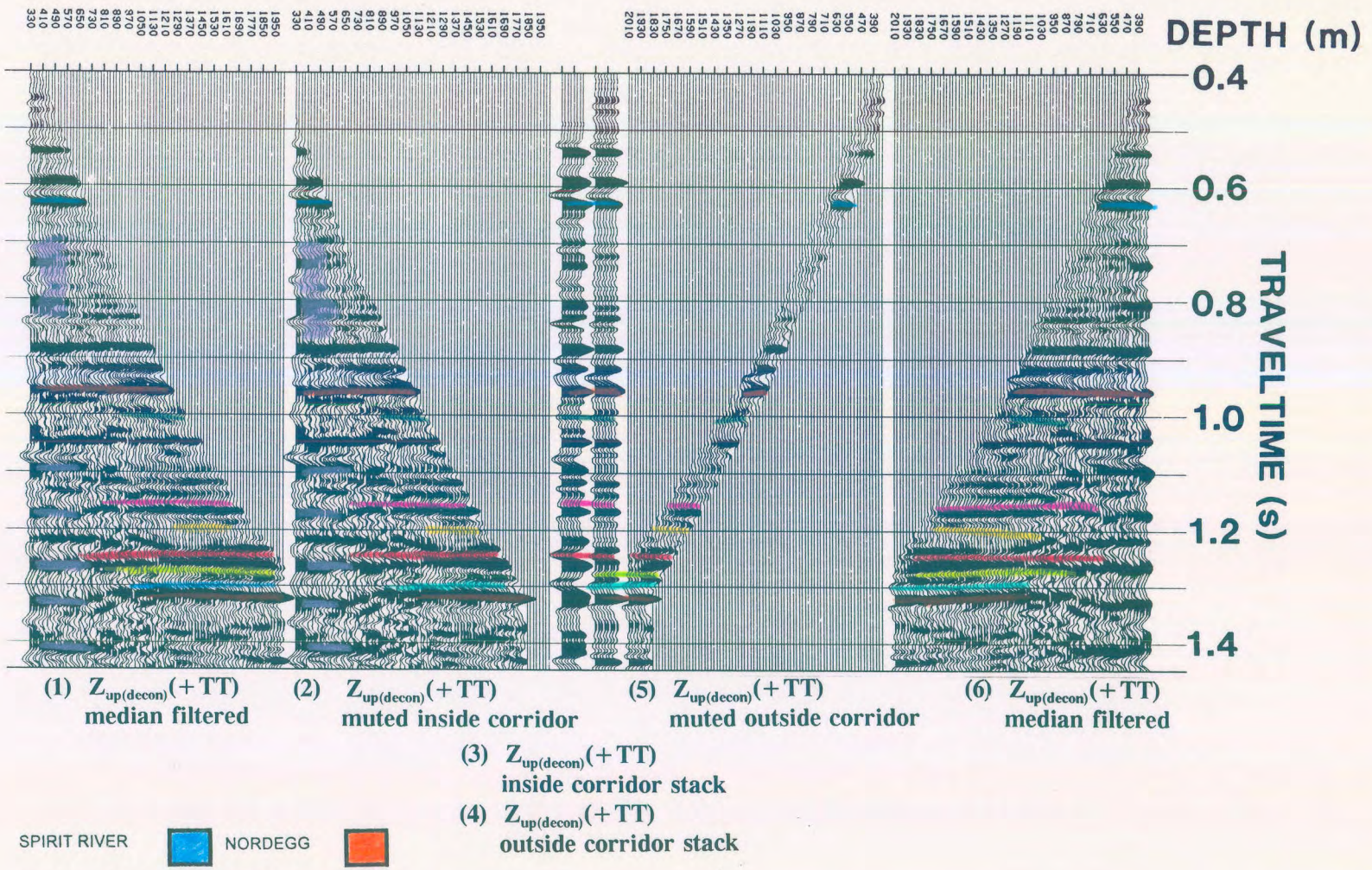

Figure 5.12 Interpretive processing panel illustrating the inside and outside corridor stacks of the $Z_{up(decon)}(+TT)$ data (from Hinds et al., 1993a).

contamination has not been completely eliminated on the shallow traces (from 1290 m to the surface). This results in a broad peak for the zone immediately above the basal Kiskatinaw (on panel 3 at 1.26 s) but the high frequency basal Kiskatinaw trough has been overpowered by residual multiple contamination. Note that the Spirit River multiple which is highlighted in purple between 0.65 and 1.0 s has been significantly attenuated on all of the traces except for the traces recorded at 490 m to the surface. The deconvolution process has given limited success; however the data can be correlated to the geology and later to the surface seismic.

5.6 Far offset VSP interpretive processing

5.6.1 Far offset data from offset FSJG1

On the far offset FSJG1 VSP data, the vertical (**Z**) and both horizontal (**X** and **Y**) axis data contain nonpartitioned elements of the upgoing and downgoing P- and SV-wavefields. Examination of the IPPs (Figs. 5.13-5.15) reveals that the partitioning of the wavefields has significant implications with respect to interpretation (Hinds et al., 1989a). The far offset IPPs for the FSJG1 data (Hinds et al., 1993a; Hinds et al., 1994c) were designed with the aim of displaying the following major processing steps:

1) hodogram-based rotation of the **X(FRT)**, **Y(FRT)**, and **Z(FRT)** data (based on windowed data enveloping the P-wave first arrival; DiSiena et al., 1984);

2) time-variant model-based rotations applied to the $\mathbf{HMAX_{up(derot)}(FRT)}$ and $\mathbf{Z_{up(derot)}(FRT)}$

data; and

3) VSP-CDP mapping (Dillon and Thomson, 1984) and Kirchhoff migration processing (Dillon, 1990; Wiggins and Levander, 1984; Wiggins et al., 1986; Wiggins, 1984) of the $\mathbf{Z''_{up}(+TT)}$ data.

5.6.2 Hodogram-based rotation; offset FSJG1

The **X(FRT)**, **Y(FRT)**, and **Z(FRT)** data for the FSJG1 far offset VSP are displayed in Figure 5.13 on panels 1, 2, and 3, respectively. The horizontal axis data (**X** and **Y**) are extremely noisy and contain only minor amounts of P-wave events. The **Z(FRT)** data contain strong downgoing P-wave events plus lower amplitude upgoing P-wave events. The hodogram-based rotation technique is designed to polarize these data so that the downgoing P-waves are presented on a single channel, **HMAX'(FRT)**.

The first step illustrated in Figure 5.13, is the hodogram-based rotation of the **X(FRT)** and **Y(FRT)** data (correcting for phase changes due to tool rotation during the movement of the sonde up the borehole). The output **HMIN(FRT)** and **HMAX(FRT)** data are displayed as panels 4 and 5, respectively. **HMIN(FRT)** and **HMAX(FRT)** data are assumed to be aligned perpendicular and tangent to the plane formed by the well and the source, respectively. Note that the **HMIN(FRT)** data (comprised of horizontally polarized shear (SH) wave events and out of the plane reflections) contains the dominant portion of the diffraction that appears at 1.0s on the 650 to 800 m traces, suggesting that the diffraction is side-swipe energy originating from a feature such as a fault out of the plane of the well and source.

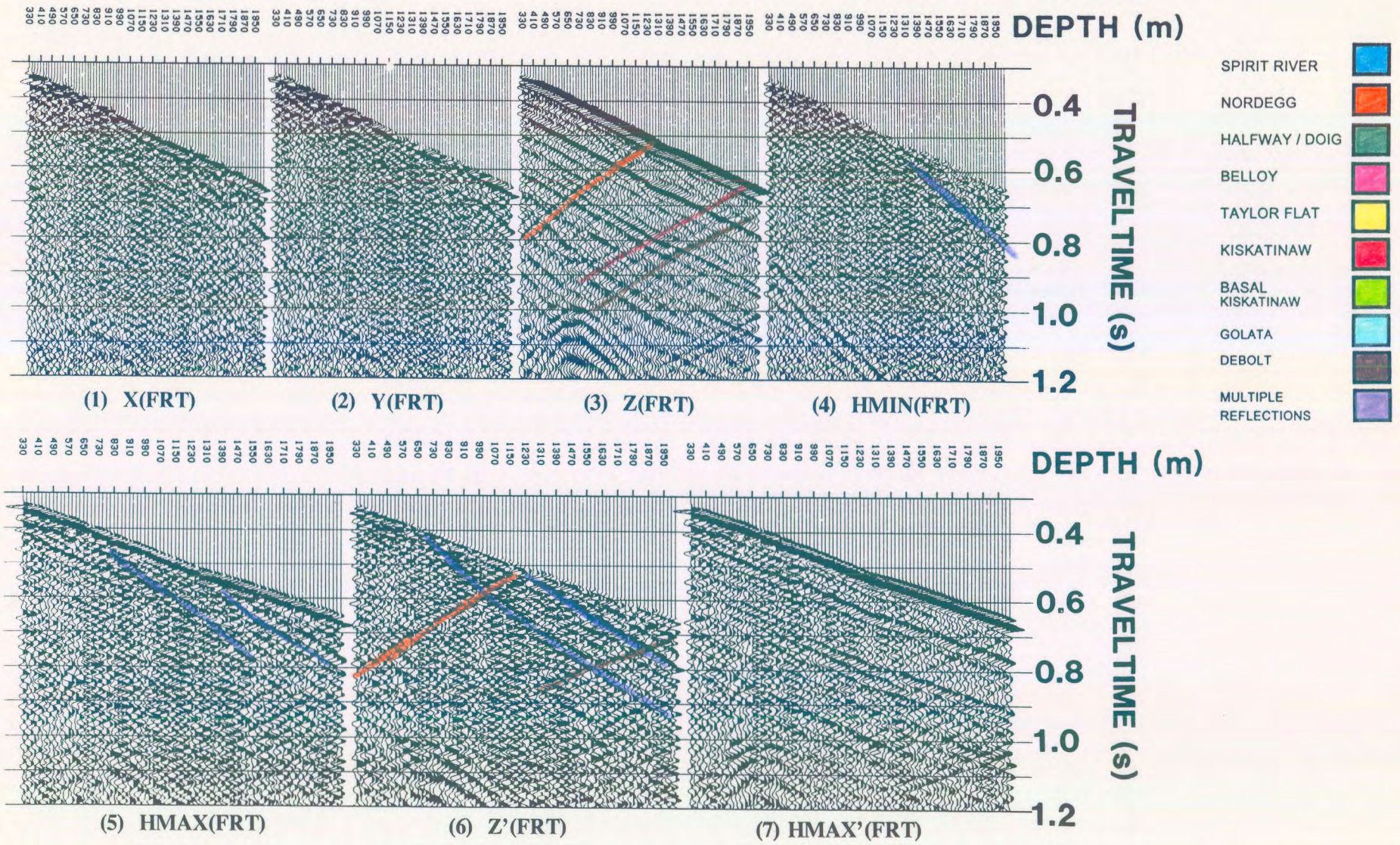

Figure 5.13 Interpretive processing panel depicting the hodogram-based rotation of the Fort St. John Graben FSJG1 far offset VSP data (from Hinds et al., 1993a).

The **Z'(FRT)** and **HMAX'(FRT)** (panels 6 and 7) data were obtained by rotating the **Z(FRT)** and **HMAX(FRT)** data using polarization angles estimated from a hodogram analysis of a window of data centred around the P-wave first arrivals of the **Z(FRT)** and **HMAX(FRT)** data (DiSiena et al., 1984). Downgoing mode-converted SV-events can be interpreted on all three axis data, **X(FRT)**, **Y(FRT)** and **Z(FRT)**. The SV-events were described for these data in chapter 2. The SV data can be used for the quality control of the second polarization; namely, **HMAX(FRT)** and **Z(FRT)** data rotating into **HMAX'(FRT)** and **Z'(FRT)** data.

The evaluation of the second polarization is based on the detection or not of SV-events (mode-converted or from any other origin) on the **HMAX'(FRT)** data. In panel 6 and 7 of Figure 5.13, the mode-converted SV events have been completely polarized onto the **Z'(FRT)** data and, at first inspection, do not appear on the HMAX'(FRT) data.

The upgoing events on VSP data can be up to 100 times weaker than the downgoing events (Hardage, 1985). The time-variant polarization IPP (Fig. 5.14) that have been designed and presented in the next section contains the wavefield separated **Z'$_{up}$(FRT)** and **HMAX'$_{up}$(FRT)** data in panels 1 and 2, respectively. It is only after the wavefield separation processing on the **Z'(FRT)** and **HMAX'(FRT)** data that the underlying upgoing event components of the **Z'(FRT)** and **HMAX'(FRT)** data can be truly evaluated.

The two sets of rotations have polarized the **X(FRT)**, **Y(FRT)** and **Z(FRT)** data so that the downgoing P-waves are effectively isolated on a single channel, **HMAX'(FRT)**, shown in panel 7 of Figure 5.13.

5.6.3 Time-variant model-based rotation: offset FSJG1

The IPP for the time-variant model-based polarization analysis for the FSJG1 offset data is shown in Figure 5.14. The **Z'$_{up}$(FRT)** and **HMAX'$_{up}$(FRT)** are shown in panels 1 and 2 (Fig. 5.14), respectively. On both panels, upgoing P-waves from the Debolt, Golata and Kiskatinaw can be clearly interpreted, indicating that the hodogram-based rotations were unsuccessful in isolating the upgoing P-wave events onto the **Z'(FRT)** panel.

In order to remove the effects of the **Z(FRT)** to **Z'(FRT)**, and **HMAX(FRT)** to **HMAX'(FRT)** transformations (which were necessary to isolate the downgoing P-waves), the **Z'$_{up}$(FRT)** and **HMAX'$_{up}$(FRT)** were derotated (using the inverse operation of the second polarization rotation). The **Z$_{up(derot)}$(FRT)** and **HMAX$_{up(derot)}$(FRT)** data, are shown as panels 3 and 4 of Figure 5.14, respectively. By inspection, the upgoing P-wave events have been effectively distributed back onto a Z-type axis data, **Z$_{up(derot)}$(FRT)**. Unlike the upgoing wave events in the **Z(FRT)** data (panel 3 in Fig. 5.13), where the downgoing P-waves were predominant, the separated upgoing P-wave events in the **Z$_{up(derot)}$(FRT)** data are dominant and interpretable.

On the **Z$_{up(derot)}$(FRT)** data (panel 3), upgoing P-waves generated by the shallow reflectors are improperly aligned (due to the choice of a single rotation angle per trace) such as the upgoing event resulting from the reflection from the Spirit River interface. These data have been derotated but the upgoing P-wave events are still partitioned on both output data (**Z$_{up(derot)}$(FRT)** and **HMAX$_{up(derot)}$(FRT)**) due to the non-zero offset of the source. The deeper events do not suffer much misalignment because the deep event raypath geometries

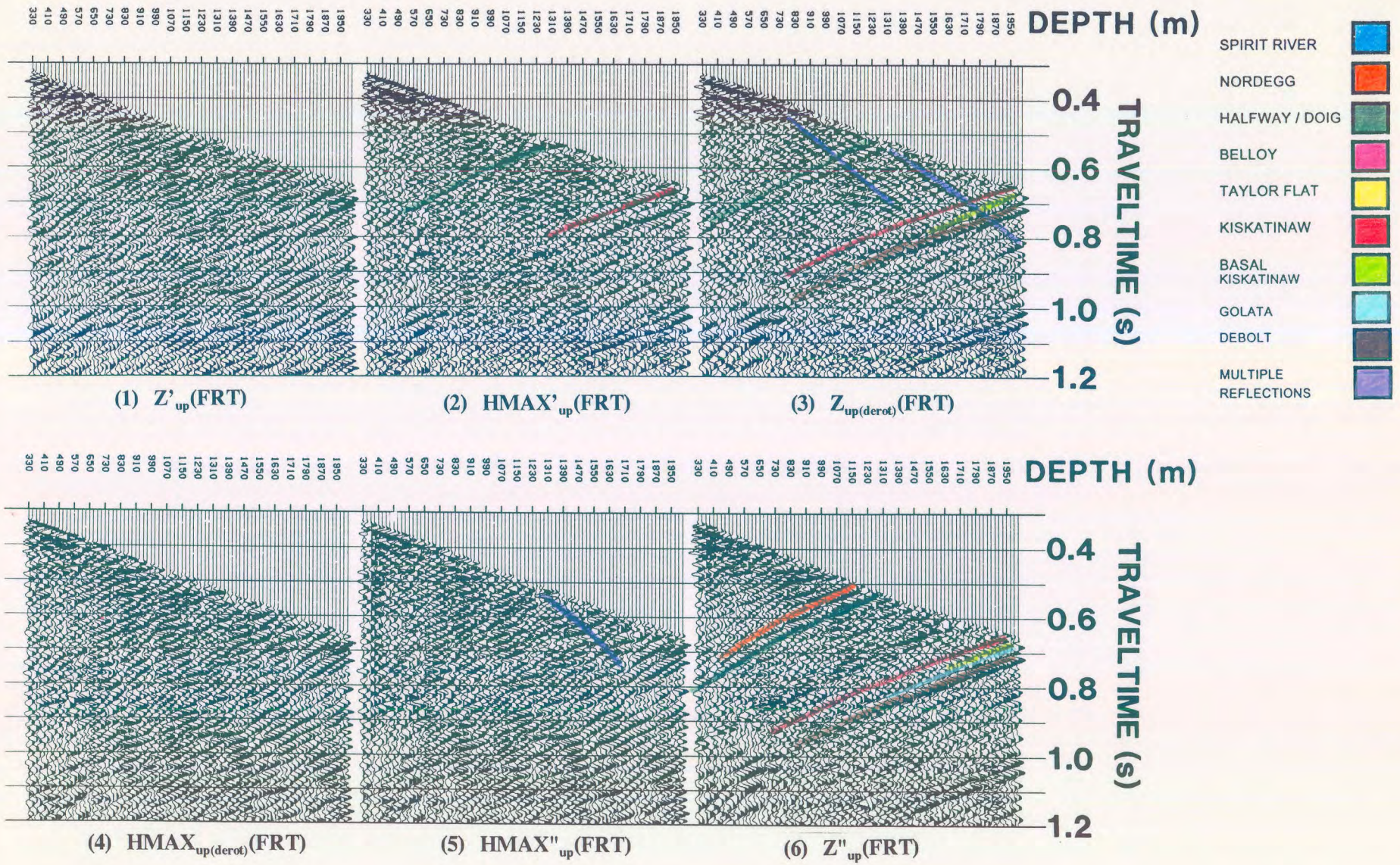

Figure 5.14 Interpretive processing panel depicting the time-variant model-based rotation of the Fort St. John Graben FSJG1 far offset VSP data (from Hinds et al., 1993a).

satisfy the near-vertical incidence angle assumption better than the raypaths of shallower events. The time-variant model-based rotation corrects for this misalignment. The output of the time-variant polarization, the **HMAX"$_{up}$(FRT)** and **Z"$_{up}$(FRT)** data, are shown in panels 5 and 6, respectively. Note that the shallow events display more alignment than on the **Z$_{up(derot)}$(FRT)** (panel 3). The rotation angle required for the Spirit River and Nordegg events on a particular trace are different to the rotation angle needed for a deeper event (such as the Debolt) on the same trace. The time-variant rotation technique (Hinds et al., 1989a) generated these different rotation angles.

The Spirit River event is barely discernable on the **Z"$_{up}$(FRT)** data because the reflected raypaths from this shallow event are at or near the critical angle. The surface-generated multiple from the Spirit River interface (observed on the nondeconvolved near offset data of panel 7 in Fig. 5.9) are significantly lower amplitude on these far offset data (panel 6; Fig. 5.13).

5.6.4 VSP-CDP mapping: offset FSJG1

Nonfiltered and median-filtered **Z"$_{up}$(FRT)** data are displayed (pseudo-two-way traveltime versus depth) in figure 5.15 as panels 1 and 2, respectively. The VSP-CDP mapped (pseudo-two-way traveltime versus offset) and Kirchhoff migrated **Z"$_{up}$(+TT)** data are shown as panels 3 and 4, respectively.

The FSJG1 offset source was located 700 m and in the direction of well 2-25. The interpretation of the surface seismic data (Fig. 5.8) suggests that a major Debolt fault

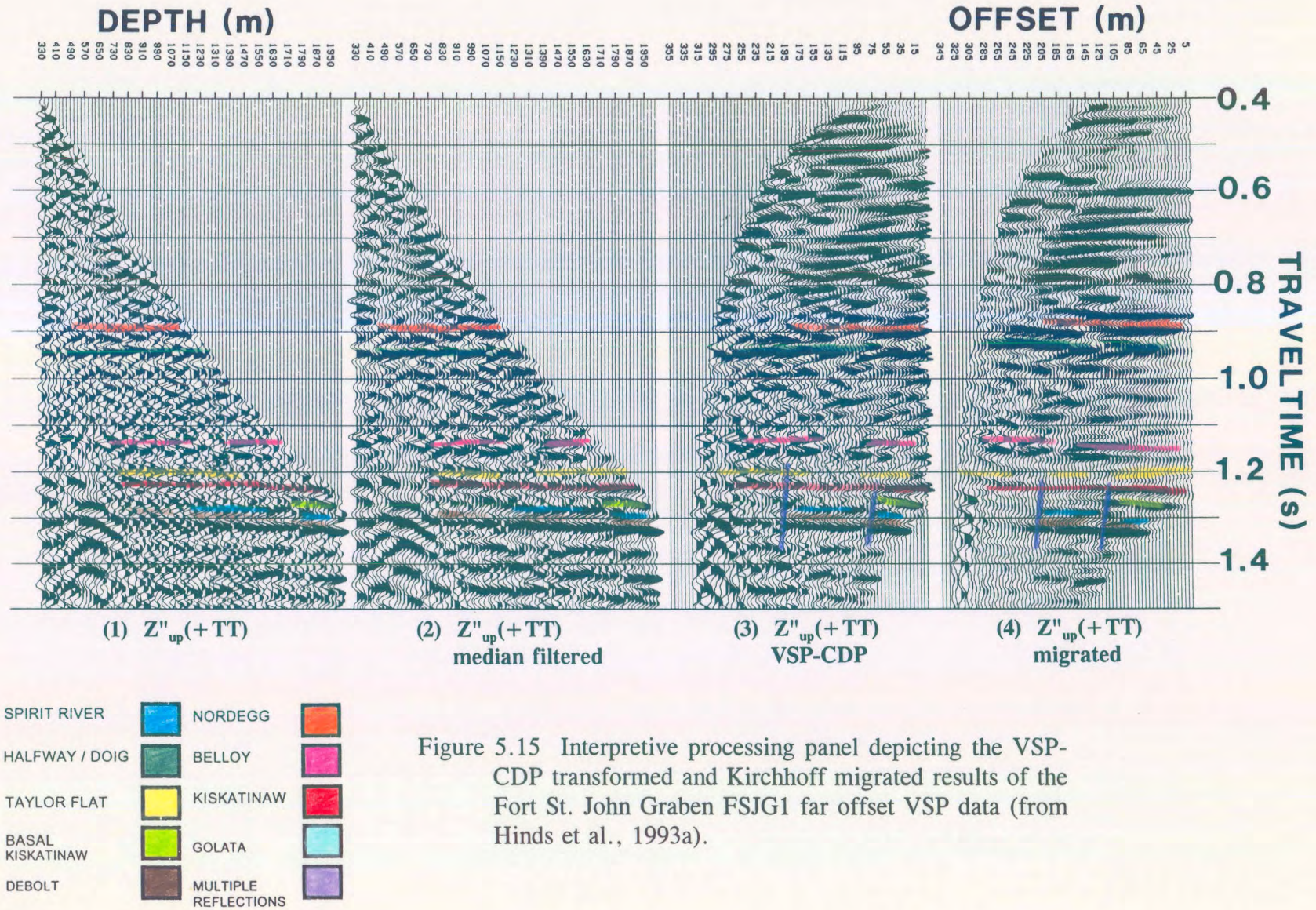

Figure 5.15 Interpretive processing panel depicting the VSP-CDP transformed and Kirchhoff migrated results of the Fort St. John Graben FSJG1 far offset VSP data (from Hinds et al., 1993a).

(displacing Debolt to the Belloy Fm material) was located between well 9-24 and well 2-25. On panels 3 and 4 (Fig. 5.15), the Debolt event on the VSP data is interpreted to be faulted in two places in between these wells; however, it is shown in section 5.7 that these VSP data image two faults not shown on the interpretation on Figure 5.8 (Hinds et al., 1994b).

A second interesting feature on panel 3 is that the signature of the basal Kiskatinaw event changes abruptly in proximity to the fault nearest well 9-24. The migrated version has smeared the event. The basal Kiskatinaw event, as interpreted, is continuous at greater offsets, but is substantially decreased in amplitude. This character change could indicate a change in lithology (increase in shale content) or porosity (increase in water content as in well 2-25).

The upper Kiskatinaw event which represents the location of the hydrocarbon reservoir within well 9-24 is interpreted on panels 3 and 4 to be laterally continuous but faulted. Vertical displacement is interpreted across two faults. This thesis is supported by geological information (Richards, pers. comm.); the upper Kiskatinaw is present in both wells 9-24 and 2-25. At well 9-24 the upper Kiskatinaw forms a gas reservoir; in the structurally higher 2-25 well this unit is nonproductive.

5.6.5 Far offset data from offset FSJG2

The FSJG2 far offset source was 741 m east of well 9-24. These data were acquired in order to map the lateral extent of the upper Kiskatinaw reservoir to the east of well 9-24, and to provide a higher resolution seismic image of faults that displace Debolt strata. The offset

survey was designed in an effort to explore a new area in which future exploration could be realized. This is a case where the VSP data capture is done before a possible seismic survey can be performed in the area. The recording and processing of these data was similar to that described for the FSJG1 survey.

In the first stage of interpretive processing, a hodogram-based rotation technique polarized the **X(FRT)**, **Y(FRT)**, and **Z(FRT)** data, so that the downgoing P-waves were presented on a single channel, **HMAX'(FRT)** as shown in Figure 5.16. The filtered output data, **Z'$_{up}$(FRT)** and **HMAX'$_{up}$(FRT)**, were derotated and time-variant model-based rotations were applied to the output data as shown in Figure 5.17. In the final stage, the **Z"$_{up}$(FRT)** data were displayed in pseudo-two-way traveltime versus depth, and in pseudo-two-way traveltime versus offset.

The **Z"$_{up}$(+TT)** data after the application of the VSP-CDP mapping are displayed in Figure 5.18. Nonmedian and median-filtered versions of the **Z"$_{up}$(+TT)** data are displayed (pseudo-two-way traveltime versus depth) as panels 1 and 2, respectively. The VSP-CDP mapped (pseudo-two-way traveltime versus offset) and Kirchhoff migrated **Z"$_{up}$(+TT)** data are shown in panels 3 and 4, respectively.

The data in panels 3 and 4 image 2 faults, both of which are of the same magnitude as those on the FSJG1 data (Fig. 5.15). The basal Kiskatinaw event is interpreted to exhibit a laterally continuous seismic signature. This is unlike the character of the basal Kiskatinaw

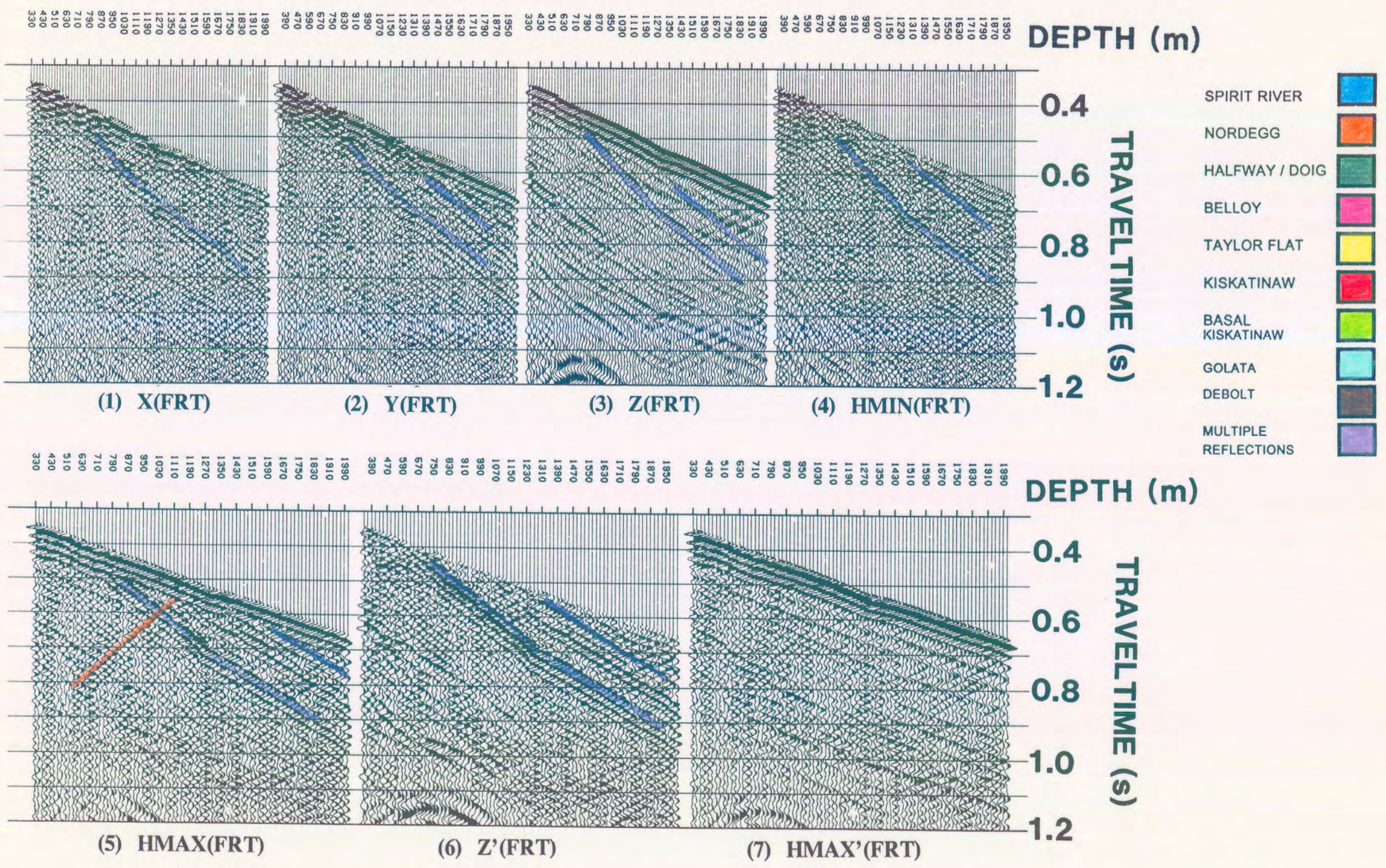

Figure 5.16 Interpretive processing panel depicting the hodogram-based rotation of the Fort St. John Graben FSJG2 far offset VSP data (from Hinds et al., 1993a).

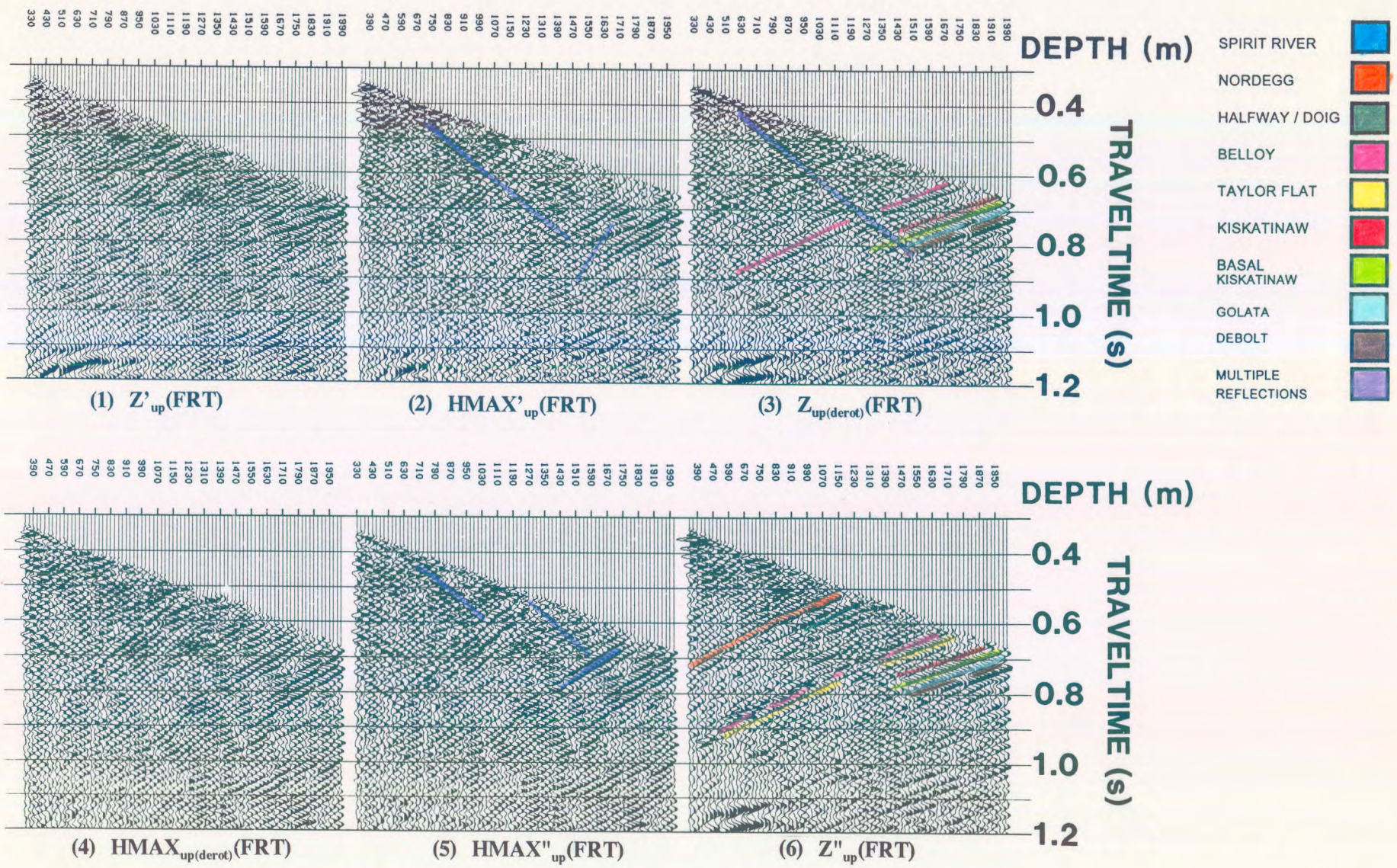

Figure 5.17 Interpretive processing panel depicting the time-variant model-based rotation of the Fort St. John Graben FSJG2 far offset VSP data (from Hinds et al., 1993a).

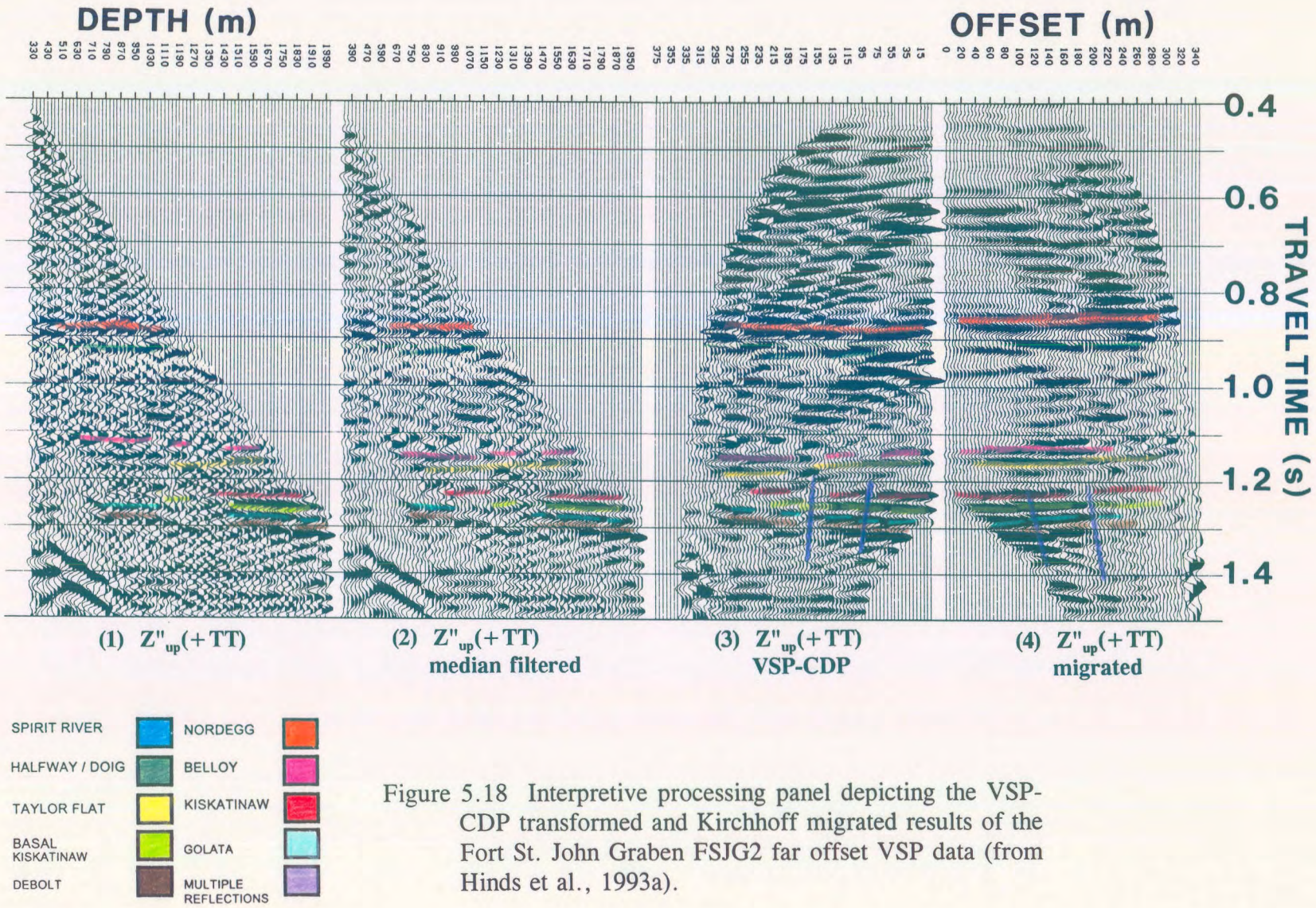

Figure 5.18 Interpretive processing panel depicting the VSP-CDP transformed and Kirchhoff migrated results of the Fort St. John Graben FSJG2 far offset VSP data (from Hinds et al., 1993a).

away from the well towards the FSJG1 offset source which decreases in amplitude beyond the first imaged fault. The upper Kiskatinaw (hydrocarbon reservoir at well 9-24), as interpreted on panel 3, is laterally continuous but faulted.

5.7 Integrated interpretation

The integrated interpretive display (IID) is shown in Figure 5.19. On the left-hand side of the IID (from Hinds et al., 1993a; Hinds et al., 1994c) in Figure 5.19, gamma ray logs for the well 9-24, well 2-25, and well 7-36 are time-tied to the current interpretation of the surface seismic data. On the right-hand side, near offset VSP data are time-tied to the gamma ray and sonic logs acquired in well 9-24. These correlated data allow for the confident interpretation of the surface seismic line and the identification of the Spirit River, Nordegg, Halfway/Doig, Belloy, Taylor Flat, upper Kiskatinaw, basal Kiskatinaw, Golata, and Debolt events. The nondeconvolved version of the VSP data is presented, in order to facilitate an analysis of multiple contamination. As evidenced by a comparison of the surface seismic line and the corridor stacks, the multiple-contaminated inside corridor stacks provide a poor tie to the data at the zone of interest (Kiskatinaw). This suggests that multiples on the surface seismic data have been effectively attenuated.

The interpretation of the surface seismic section that incorporates the VSP information (normal polarity display; Fig. 5.20) differs slightly from the pre-well interpretation (Fig. 5.8). Of particular significance is that on the updated version, the Taylor Flat and Kiskatinaw events are confidently correlated. Note that in the post-VSP interpretation, the Taylor Flat event is absent at well 7-36. This interpretation is supported by the well log

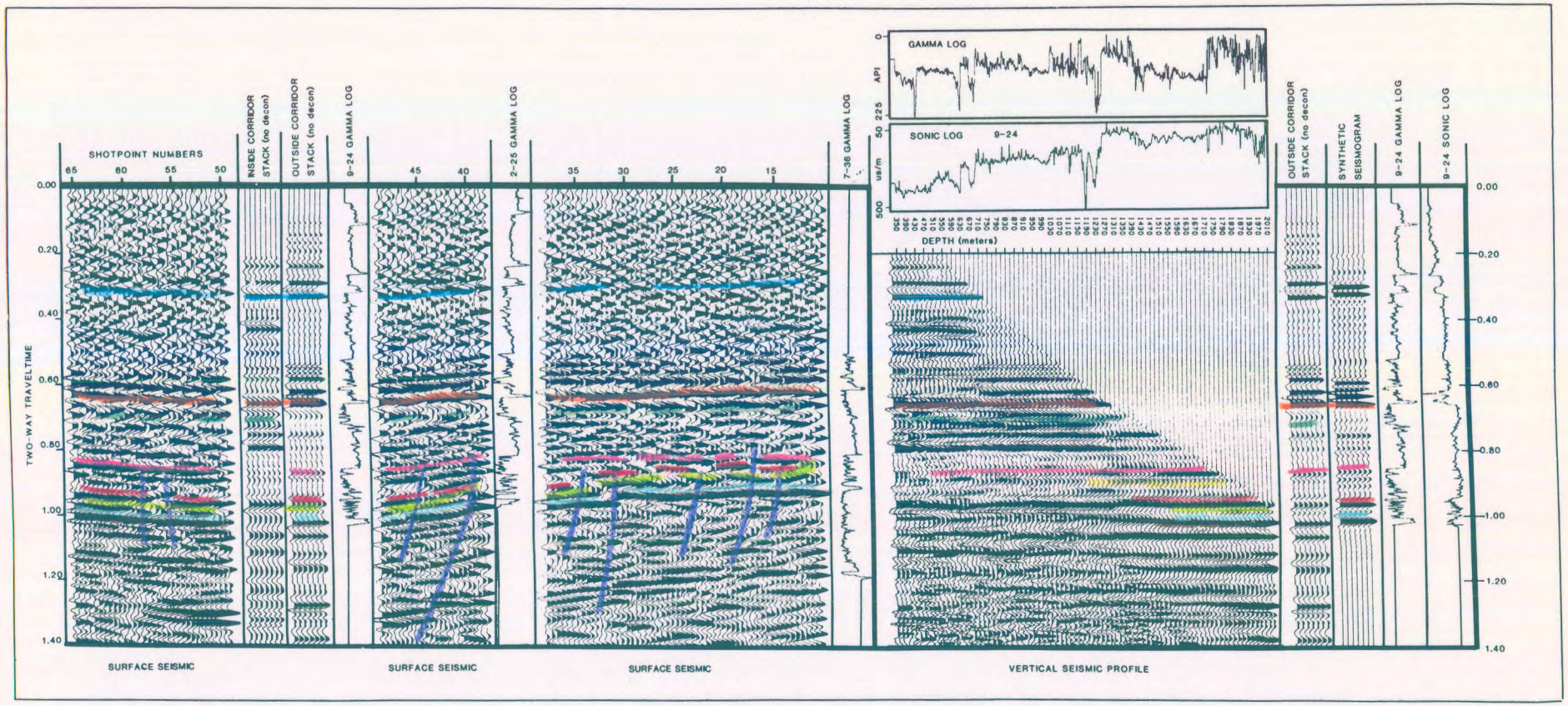

Figure 5.19 Integrated interpretive display of the Fort St. John Graben exploration data (from Hinds et al., 1993a).

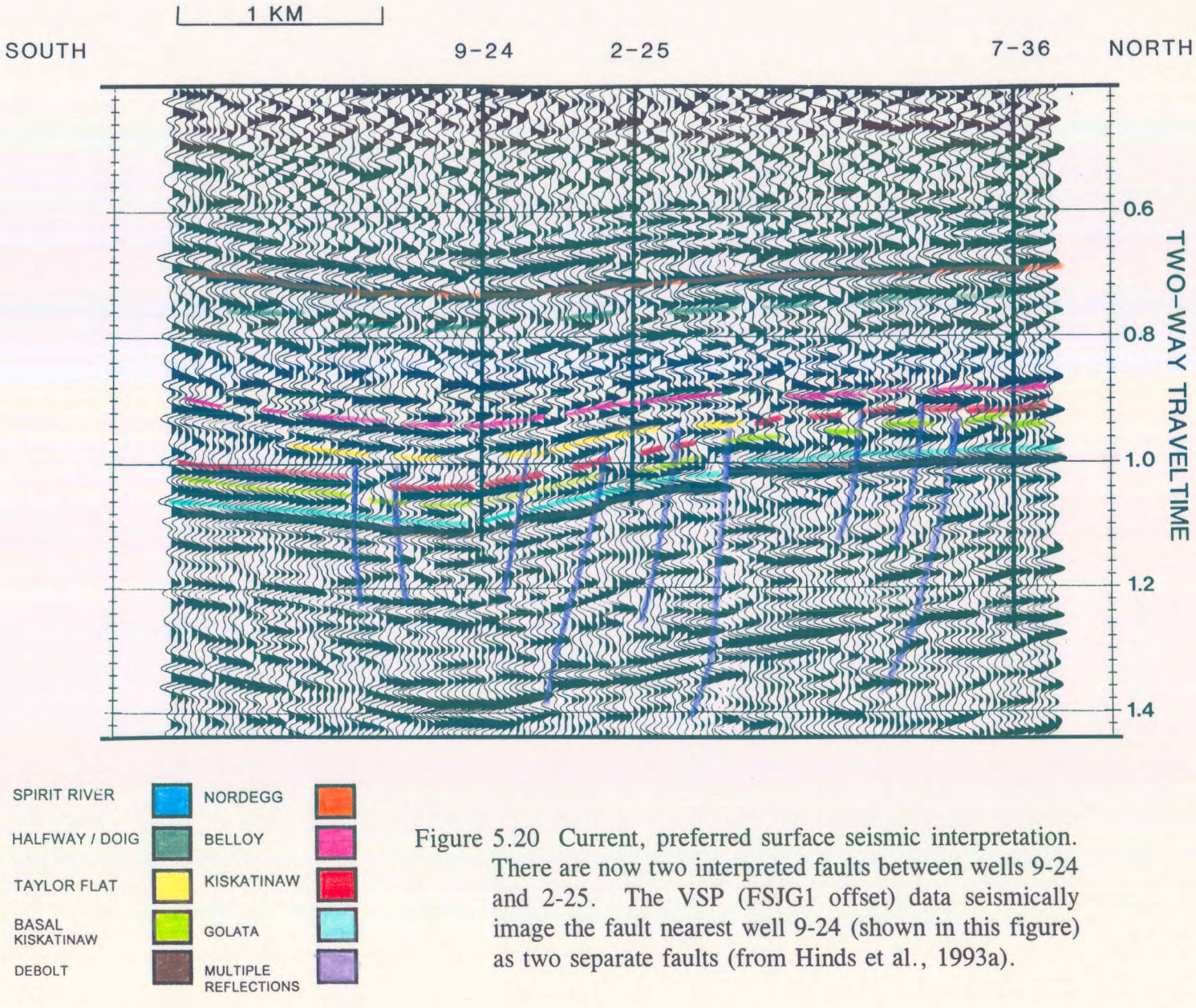

Figure 5.20 Current, preferred surface seismic interpretation. There are now two interpreted faults between wells 9-24 and 2-25. The VSP (FSJG1 offset) data seismically image the fault nearest well 9-24 (shown in this figure) as two separate faults (from Hinds et al., 1993a).

control.

The geologic cross-section of Figure 5.21 was constructed on the basis of the post-VSP interpretation of the surface seismic line and the analysis of the far offset VSP data. It is consistent with the well log, surface seismic and seismic profile control. Up-to-date information using conodont research and lithostratigraphic data (Richards, pers. comm.) is shown in Figure 5.21 as Upper Carboniferous strata informally known as the Ksituan Member of the Taylor Flat Formation (Hinds et al., 1994b and Hinds et al., 1994c). This geologic cross-section is an update to the one presented in Hinds et al. (1993a) and is discussed in Hinds et al. (1994b) and Hinds et al. (1994c).

A discrepancy that arose and was resolved in Hinds et al. (1994b) came about from the observation that there are two faults interpreted on the VSP-CDP data shown in Figure 5.15 and three faults between well 9-24 and well 2-25 on the geologic cross-section shown in Figure 5.21. In addition, on the reinterpreted seismic data, shown in Figure 5.20, there are two faults interpreted between wells 9-24 and 2-25. The two faults interpreted on the VSP-CDP data do not correlate with the interpreted fault shown on Figure 5.8 (between wells 9-24 and 2-25); these interpreted faults (Fig. 5.15) are represented on the reinterpreted seismic data (Fig. 5.20) as a single fault near to well 9-24. The surface seismic data could not resolve the seismic expression of the fault into two separate images as seen on the VSP-CDP data (Fig. 5.15).

In Hinds et al. (1994b), a plan view of the FSJG1 source offset position along with the location of the two VSP interpreted faults and surface seismic located fault (near well 2-25)

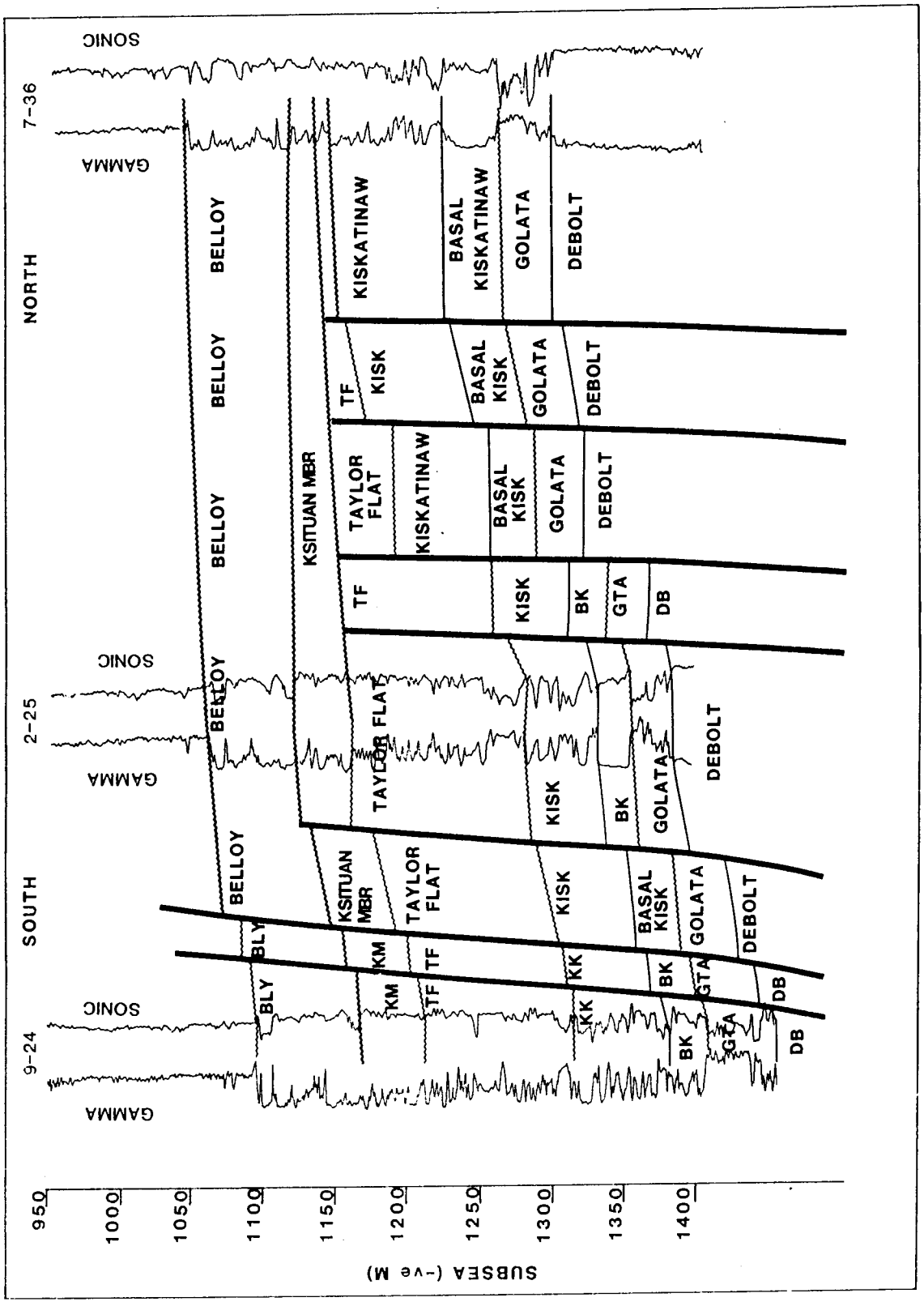

Figure 5.21 Geologic cross-section incorporating information from the surface seismic, VSP and geologic well log results (from Hinds et al., 1994c). Note that three faults have been postulated to be between wells 9-24 and 2-25.

was discussed and is shown in Figure 5.22 (Hinds et al., 1994c). This presentation of the VSP and surface seismic line geometry aids in the resolution of the discrepancy discussed in Hinds et al. (1994b). In Figure 5.22, well 9-24 is located due East of CDP number 49 of the seismic line shown in Figures 5.8 and 5.20. The far offset source location is marked by a circle to the northwest of the well 9-24 location. The subsurface coverage of the VSP-CDP data extends along a direction towards the offset source location starting at well 9-24 out to half the distance from well 9-24 to the source. The two VSP illustrated faults on the seismic line nearest well 9-24 project onto the seismic line at CDP numbers 47 and 48. These faults are shown as a single fault on the reinterpreted seismic line in Figure 5.22. The layout in Figure 5.21 clearly shows that the fault displayed on the seismic line immediately South of well 2-25 is not imaged on the VSP-CDP data; only on the seismic data. In this case, the VSP-CDP interpretation has brought new information into the integrated interpretation.

5.8 Conclusion

The exploratory well 9-24 was drilled on the downthrown side of a fault block on the basis of conventional surface seismic data. The expectation was that the gas-prone sandstones of the basal Kiskatinaw Fm would be truncated laterally and sealed against the upthrown fault-block. Contrary to expectations, the basal Kiskatinaw was unproductive; however, well 9-24 did encounter commercial gas within the upper Kiskatinaw which was now shut-in.

Figure 5.22 Plan map of the FSJG1 offset source area showing the fault locations as interpreted from the VSP and surface seismic data (from Hinds et al. 1994c). The VSP data (FSJG1 far offset) imaged the two faults along the seismic line nearest to well 9-24 and the seismic imaged the fault nearest to well 2-25. These two datasets complement each other in the construction of the geological interpretation shown in Figure 5.21.

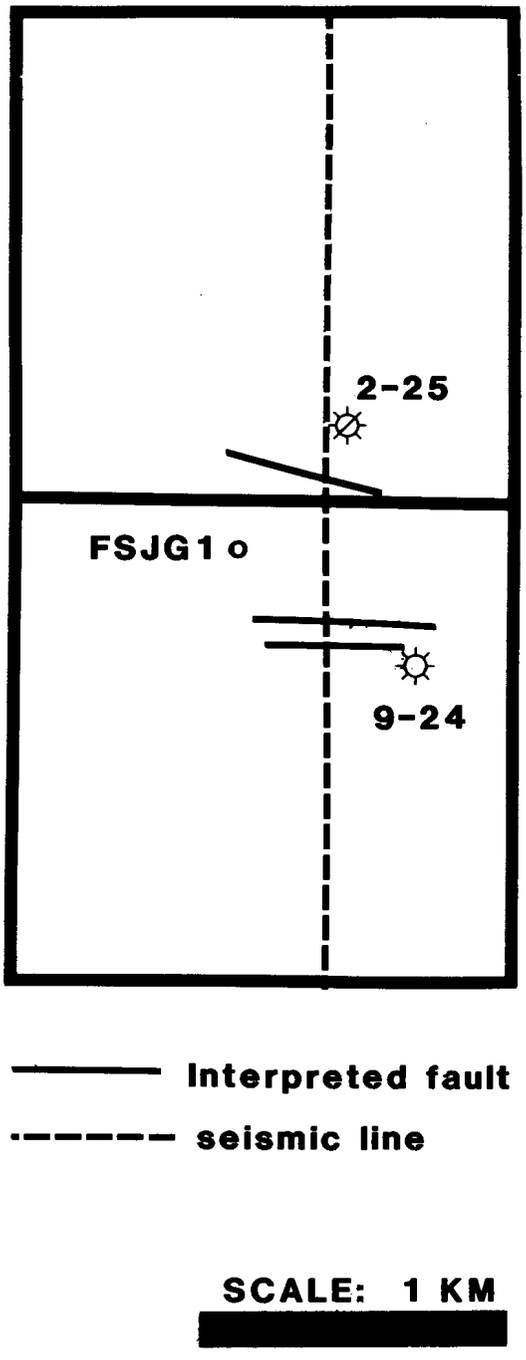

To obtain a high resolution seismic image of the subsurface in the vicinity of well 9-24, and to evaluate the proximity of any displacements features such as faults which might not have been resolved on the surface seismic data, three VSP surveys were designed and run on the 9-24 well-site. This seismic profiling information, in conjunction with surface seismic coverage, was used to image the subsurface fault pattern, and elucidate the seismic signature and lateral continuity of the upper Kiskatinaw Fm strata. The profile data supplemented the surface seismic and well log control in that VSP data could be directly correlated to the surface seismic data. As a result, the surface seismic control could be accurately tied to the subsurface geology; multiples could be identified on the VSP data and evaluated on the surface seismic data; and the subsurface, in the vicinity of the borehole, was better resolved on the VSP data than on the surface seismic control.

The information provided by the VSP surveys allowed this work to provide a refinement of the interpretation of the surface seismic data, and enabled the construction of a detailed geologic cross-section (Fig. 5.21). These interpretations provide information with respect to the subsurface in proximity to well 9-24, and perhaps more importantly, further elucidate the geologic history of the structurally complex Fort St. John Graben area (Richards et al., 1994).